January 2021 Volume 3 Issue 1

## Journal of Marine Science























#### Editor-in-Chief

#### Dr. Euge Victor Cristia RUSU

University Dunărea de Jos of Galați, Romania

#### **Editorial Board Members**

Ladan Momayez, Canada

Roya Jahanshahi, Iran

Shah Iram Niaz, Pakistan Xinming Lei, China

Leão Martins José Manuel, Spain Yongfu Li, China

> Chinmay Bhat, India Jinpei Yan, China

Ma Pilar Cabezas, Portugal Bei Huang ,China

Weiwei Bai, China Anan Zhang, China Christos Kastrisios, United States Run Liu, China

Erick Cristóbal Oñate González, Mexico Prabhakar G., India

Cataldo Pierri, Italy M.Masilamani Selvam, India

Amzad Hussain Laskar, Netherlands Ramesh Chatragadda, India

Mohammed Ali Mohammed Al-Bared, Malaysia Alison Kim Shan Wee, China

> Sivasankar Palaniappan, India Raouia GHANEM, Tunisia

Surya Prakash Tiwari, Saudi Arabia Milton Luiz Vieira Araujo, Brazil

Minao Sun, China Sergio Chazaro Olvera, Mexico

Nima Pourang, Iran Imad Mahmood Ghafor, Iraq

Rossana Sanfilippo, Italy Blanca Rincón Tomás, Germany

Saif Uddin, Kuwait Alireza Bahramian, Iran

Ali Pourzangbar, Italy Mohd Adnan, Saudi Arabia

Jonathan Akin French, United States Riyad Manasrah, Jordan

> Linyao Dong, China Tunde Olukunmi Aderinto, United States

> > Valeria Di Dato, Italy

Mostafa Hassanalian, United States

A. Sundaramanickam, India Fathy Ahmed Abdalla, Egypt

Marina Vladimirovna Frontasyeva, Russian Federation

Achmad Fachruddin Syah, Indonesia Hitoshi Sashiwa, Japan

Cheung-Chieh Ku, Taiwan Moussa Sobh Elbisy, Egypt

Maryam ShieaAli, Iran

Ta Bi Ladji Samuel, Côte d'Ivoire Abdolreza Karbassi, Iran

Samia Saad Abouelkheir, Egypt Ali Altaee, Australia

> Yong Lin, China Venko Nikolaev Beschkov, Bulgaria

Qiulin Liu, China Şükran Yalçın Özdilek, Turkey

Phan Minh-Thu, Vietnam Chunhui Tao, China

Abdelali Achachi, Algeria Kyungmi Chung, Korea

Sergio Chazaro Olvera, México Min Du, China

Krzysztof Czaplewski, Poland Asunción Baquerizo, Spain

Rachael Ununuma Akpiri, United Kingdom Mohd Hazmi bin Mohd Rusli, Malaysia

> Tim Frazier, United States Seshagiri Rao Kolusu, Brighton

Daniel Ganea, Romania Zaman Malekzade, Iran

Bo Zhou, China Neelamani Subramaniam, Kuwait

Vittal Hari, Germany

# Journal of Marine Science

**Editor-in-Chief** 

Dr. Euge Victor Cristia RUSU





Volume 3 | Issue 1 | January 2021 | Page1-47

#### **Journal of Marine Science**

#### **Contents**

#### **ARTICLE**

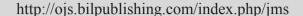
- 1 Numerical Simulation of Resistance Field of Hull-Propeller-Rudder Coupling
  - Hong Xie Baoji Zhang
- 8 An Evaluation of the Main Physical Features and Circulation Patterns in the Black Sea Basin
  - Alina Girleanu Eugen Rusu
- 19 Research on Marine Pollution Problems and Solutions in China from the Perspective of Marine Tourism
  - Yuxiang Zheng Dandan Liu
- 29 Microbial Communities in Water during Red Tides along the Coast of China-A Case Study of
  - Prorocentrum Donghaiense Red Tide in the East China Sea
  - Bei Huang Na Wei Yuheng Hu Hongyue Mao
- 39 Mass Spectrometry-based Sequencing of Venom Peptides (Conotoxins) from Vermivorous Cone Snail,
  - Conus Loroisii: Toxicity of its Natural Venom
  - Humaira Saleh Syed Rishimol R Arun Kumar J M Masilamani Selvam Rajesh R P

#### Copyright

Journal of Marine Science is licensed under a Creative Commons-Non-Commercial 4.0 International Copyright (CC BY- NC4.0). Readers shall have the right to copy and distribute articles in this journal in any form in any medium, and may also modify, convert or create on the basis of articles. In sharing and using articles in this journal, the user must indicate the author and source, and mark the changes made in articles. Copyright © BILIN-GUAL PUBLISH-ING CO. All Rights Reserved.



#### **Journal of Marine Science**





#### ARTICLE

## Numerical Simulation of Resistance Field of Hull-Propeller-Rudder Coupling

#### Hong Xie Baoji Zhang\*

College of Ocean Science and Engineering, Shanghai Maritime University, Shanghai, 201306, China

#### ARTICLE INFO

Article history

Received: 27 October 2020 Accepted: 18 November 2020 Published Online: 31 January 2021

Keywords:
RANS method
Hull-propeller-rudder
Resistance
Numerical simulation

#### ABSTRACT

Based on the incompressible RANS equation, the KVLCC1 ship's resistance field's numerical simulation is carried out. In this paper, the bare hull (calm water resistance and wave resistance) and hull-propeller-rudder models are studied and compared with the values of the Hydrostatic resistance test. In the hull-propeller-rudder system's performance analysis, the body force method is used to replace the real propeller model. The new calculation domain is set for the hull-propeller-rudder system model and meshed again to obtain the highly reliable numerical simulation results. Finally, the calculation results are analyzed. The research results in this paper can provide technical support for the resistance of similar ship types.

#### 1. Introduction

The commonly used methods for studying the hydrodynamic performance of ships are tank experiments and numerical simulation. Because of the high cost and the long cycle time of the tank experiment, it is difficult for individual researchers. Therefore, most scholars currently use numerical simulation. In recent years, the use of the CFD (Computational Fluid Dynamics) method has been used to study the hydrodynamic performance of ships and has achieved rich research results [1-2]. There are three types of ship hydrodynamic performance: resistance prediction of the bare hull in still water, performance prediction of ship self-propulsion, and ship-propeller-rudder system performance prediction. Especially, the bare hull's hydrostatic resistance prediction has been studied very maturely, and the error with the experimental value is kept within 3%,

which can meet the requirement of engineering <sup>[3]</sup>. Although the performance prediction of ship self-propulsion mainly calculates the propeller's hydrodynamic performance and many researchers <sup>[4]</sup>, due to the complexity of resistance prediction of the ship-propeller-rudder system, there are few researchers right now. However, the various analyses under the hull, propeller, and rudder interaction are currently a hot topic in ship hydrodynamics.

Due to the mutual coupling, a complicated circumferential flow field will be generated in the waters. On the one hand, the propeller's suction effect will change the flow field at the stern and the pressure on the surface of the hull, thereby increasing the resistance. On the other hand, when the flow field at the stern of the hull changes, it will affect the propeller's thrust. It is very likely to form the cavity, noise, etc. Also, it can change the rudder's side load. Specifically, when the propeller produces an explo-

Baoji Zhang,

College of Ocean Science and Engineering, Shanghai Maritime University, Shanghai, 201306, China;

Email: zbj1979@,163.com

<sup>\*</sup>Corresponding Author:

sive wake field for the rudder, its lift will be severely damaged. This paper studies the KVLCC1 ship-propeller-rudder system's resistance performance based on the CFD because of the previous research results. The research results can provide a meaningful reference for the design and calculation of similar ship types.

#### 2. Basic Theory of CFD

The entire flow field uses the continuity equation and the Navier-Stokes equations as the governing equations [5]. It uses the turbulence model, adopts the VOF (Volume of Fluid) method to track the free surface. Besides, the governing equation is discretized by the volume-centered finite difference method. All time-term are used in the Second-order backward difference method; wave generation methods use the boundary velocity method.

Wave equation:

$$\eta = a\cos(kx - \omega_e t)$$
 (1)

Velocity Field:

$$u(x, y, t) = a\omega_0 e^{kz} \cos(kx - \omega_e t) + U$$
(2)

$$v(x,y,z) = 0 (3)$$

$$w(x, y, z) = a\omega_0 e^{kz} \sin(kx - \omega_z t)$$
(4)

Where the k is the wavenumber, which depends on the formula:  $k=2\pi/\lambda$ ; the  $\omega_0$  is the Natural frequency of waves. It depends on the recipe:  $\omega_0=\sqrt{2\pi g/\lambda}$ .

The establishment of the damping region is necessary for preventing the influence of the reflected wave. The damping model provided by STAR-CCM+ is used to dampen the waves. The length of the damping region is 1-2 times the steady wave-making. In this paper, by adding a damping term <sup>[6]</sup> at the outlet of the pool to attenuate the wave in the vertical direction, the vertical velocity at the outlet of the numerical wave pool is almost zero to achieve the purpose of wave elimination. The wave dissipation formula is deduced as follows:

$$s_z^d = \rho(f_1 + f_2|w|) \frac{e^{\kappa} - 1}{e^1 - 1} w$$
 (5)

where, 
$$k = \left(\frac{x - x_{sd}}{x_{ed} - x_{sd}}\right)^{n_d}$$
,  $x_{sd}$  is the starting point of the

absorbing region,  $x_{\rm ed}$  is the outlet boundary of the wave tank,  $f_1, f_2$  and  $n_{\rm d}$  are the parameters of the model, and  $\beta$  is the vertical velocity component.

#### 3. Motion Equation of Ship with 6-DOF

When establishing the ship model's 6-DOF motion equations, it is necessary to establish two reference frames: one is the fixed coordinate system, O<sub>o</sub>X<sub>o</sub>Y<sub>o</sub>Z<sub>o</sub>.

and the other is the follow-up coordinate system GXYZ fixed on the hull. As shown in Figure 1, the origin of the moving coordinate system is at the center of gravity of the ship, in which the Gx, Gy, and Gz are the intersections of the midship section, the longitudinal section in the center plane, and the waterplane passing through the center of gravity, respectively. Follow-up coordinate system, the X-axis is positive for the bow, the Y-axis is positive for the starboard side and the Z-axis is positive for the downward direction [7]. The STAR - CCM + FDB module activates the heaving and pitching, to complete the ship motion simulation performance.

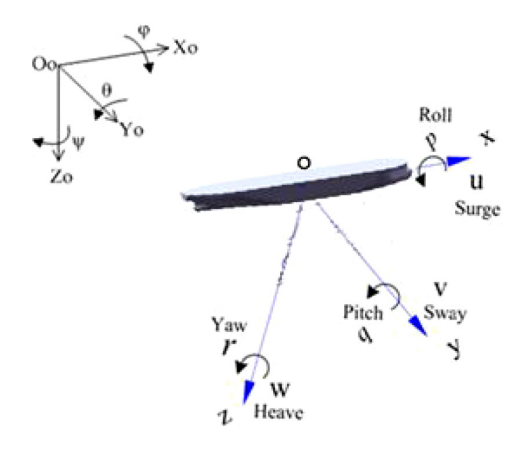


**Figure 1.** The fixed coordinate system and the follow-up coordinate system

$$\frac{\mathrm{dB}}{\mathrm{d}\,t} + \Omega \times B = F \tag{6}$$

$$\frac{\mathrm{dK}}{\mathrm{d}\,t} + \mathbf{\Omega} \times K + U \times B = M \tag{7}$$

Where the B,  $\Omega$ , F, K, U, and M, in turn, are the moment of the resultant force, ship's momentum, angular velocity, external force, the moment of momentum, and ship speed, respectively.

#### 4. KVLCC1 Ship Hull

The KVLCC1 ship model is the standard ship type in the international symposium SIMMAN2014. Compared with the ship types such as Wigley and KCS, its surface is more complicated. To compare the numerical simulation results with the experimental values, the scale ratio used in the model is 64.386 (compared with the actual ship model). The 3D model is shown in Figure 2, and the concrete parameters are shown in Table 1.

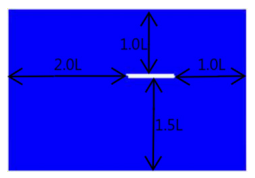


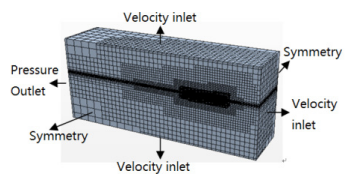
Figure 2. 3D model of KVLCC1 naked hull

**Table 1.** The main parameters of the KVLCC1 ship model

Parameters	Numerical	Parameters	Numerical
The length between perpendiculars(m)	4.97	Block coefficient, Cb	0.8099
Molded breadth, B(m)	0.901	Froude number, Fn	0.142
Draft, Td(m)	0.323	Speed, Vm(m/s)	0.994
Wet-surface area, S(m2)	6.589		

The computational domain and boundary of the KVL-CC1 ship model are shown in Figure 3. Among them, the inlet is defined as the velocity inlet; the outlet is defined as the pressure outlet. Also, the two sides are set as the plane of symmetry. The other positions are set as the velocity inlet; the hull is a no-slip wall. In order to save computing resources, only half of the hull is simulated.





(a) Computational domain

(b) Boundary setting

**Figure 3.** The computational domain and boundary conditions

For the computational domain grid, set the raw size to 0.1m, the prism layers number is 6, and the absolute thickness values to be 0.002m. The thickness of the boundary layer grid's height value mainly depends on the Reynolds number. When dividing the grid, the parameter y+ refers to the first boundary layer grid, which is generally controlled at about 6.25 to 50. It is obtained from the dimensionless local Reynolds number in the near-wall region. The estimating formula is:

$$y^{+} = 0.172 \left(\frac{y}{L}\right) \text{Re}^{0.9}$$
 (8)

Mesh generation is an essential part of numerical simulation. The quantity and quality of the grid will significantly affect the time and results of the numerical simulation calculation. Furthermore, the mesh's quality plays a decisive role in calculation accuracy. To better simulate the hull's motion on the waves, this paper adopts the chimera grid technology that comes with Star-ccm to establish the background (fixed part) grid and overlapping (moving part) grid area, respectively. The background grid is relatively sparse, and the overlapping regions are denser. Overlapping and background grids must be excessive in a particular proportion. The free surface must also

ensure that there are at least 80 grids within a wavelength and at least 20 grids within a wave height. Taking into account computing time and machine location, the final number of grids generated is 2.49 million. Figure 4 shows the mesh generation of the hull and rudder's surface and the mesh refinement of the bow and stern on the ship. From the figures, it can be seen that the grid near the free surface gradually becomes sparse outward from the hull. To capture the free surface more accurately, the water surface also needs to be refined, as shown in Figures 5, 6.

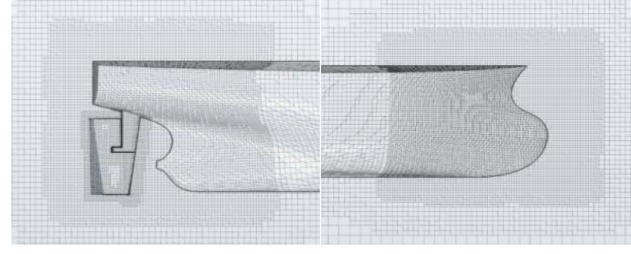




Figure 4. Hull meshing

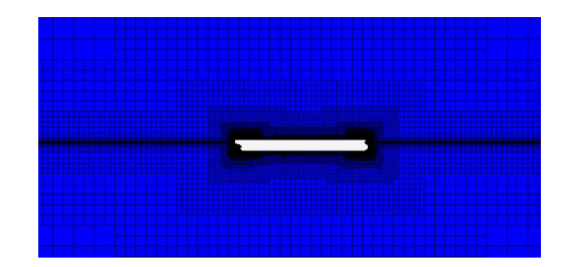


Figure 5. Free surface and boundary layer meshing

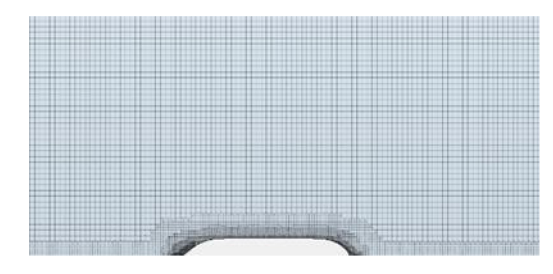


Figure 6. The grid of water surface

#### 5. Hydrostatic Resistance Calculation

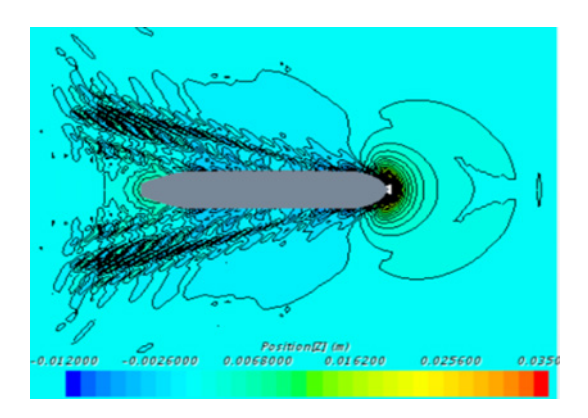
When Fn=0.142, the iteration number reaches 1249, so at 5s, the pressure curve stabilizes. The iteration number from 14492 to 17,489, the resistance change rate is less than 5% and stable at 6.612N (only half of the models are selected in the simulation; the entire ship's resistance must be multiplied by 2). Finally, the total number of iterations

	Table 2. Com	parison of	calculation	values with	experimental	values (	(N)	)
--	--------------	------------	-------------	-------------	--------------	----------	-----	---

$F_n$	Result	Pressure drag	Frictional resistance	Total resistance	Deviation between total resistance and experimental value
0.142	Calculated value	1.023	12.20	13.224	-4 64%
0.142	Experimental value	-	-	13.867	-4.0470

is 24,735. This simulation uses an eight-core workstation to calculate, which is about wall clock time 12 hours. Compare the calculation results with the experimental results [8], as shown in Table 2. It can be seen from the table that the calculation result is relatively close to the experimental value, indicating that the reliability of the simulation result is higher.

Figure 7 is the oscillogram of the free surface of the bare hull. It can be seen from the oscillogram that the stabilized waveform shows the shape of the Kelvin wave. Figure 8 shows the pressure distribution on the surface of the bare hull in still water. According to Figure 8, it can be seen from the figure that the pressure in the stagnation area formed at the bow decreases from the maximum. Also, vortices are generated at the bilge and shoulder, which causes the pressure to decreases rapidly and forming two low-pressure regions. There was almost no change in pressure in the mid-hull area. In the middle and rear part of the hull, the pressure first drops until it rises to a certain extent at the stern, mainly due to shoulder waves and vortices' influence.



**Figure 7.** The oscillogram of the free surface of the bare

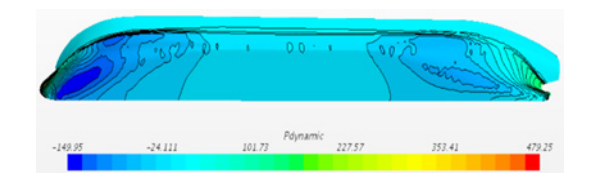


**Figure 8.** The pressure profile of the free surface of the bare hull

#### 6. Wave Resistance

The calculation conditions of wave resistance are shown in Table 3. Compared with the drag convergence curve in still water. When the calculation time step is set the same, the time required for the bare hull model's resistance to reach convergence in the first-order regular wave becomes significantly longer. Similarly, when the number of iterations is 2501, that means the physical time is about 10s. At this time, it tends to be stable. Then, when the iteration number is between 5096 and 6019, the value change range is less than 5% and finally stabilizes at 7.86N. The time history curve is shown in Figure 9. Comparing the value with the resistance of the bare hull in still water and the experimental data, as shown in Table 4, it can be found that the resistance in the first-order regular wave is increased by 13.36% compared with the resistance of the bare hull in still water. As can be seen that waves have a significant influence on hull resistance.

The wave added resistance is equal to wave resistance minus the calm water resistance,

$$R_{aw} = R_W - R_T \tag{9}$$

Where the Raw,  $R_W$  and  $R_T$  are the wave added resistance, the wave resistance and calm water resistance, respectively.

The dimensionless expression of the wave added resistance is:

$$C_{aw} = \frac{R_{aw}}{0.5\rho SV^2} \tag{10}$$

Where the  $\rho$ , S and V are the fluid quality density, the hull wet surface and speed, respectively.

**Table 3.** Calculation conditions

Parameters	Numerical
Froude number, F <sub>n</sub>	0.142
Wave steepness, ak	0.0109
Wavelength, $\lambda(m)$	2.485
Wave height, H(m)	0.0487
Frequency, v(Hz)	0.2234

**Table 4.** Comparison of wave resistance with experimental values (N)

$F_n$	Results	Hydrostatic resistance	Wave resistance	Deviation between Hydrostatic resistance and Wave resistance
0.142	Calculated value	13.224	15.720	12.200/
0.142	Experimental value	13.867		13.36%

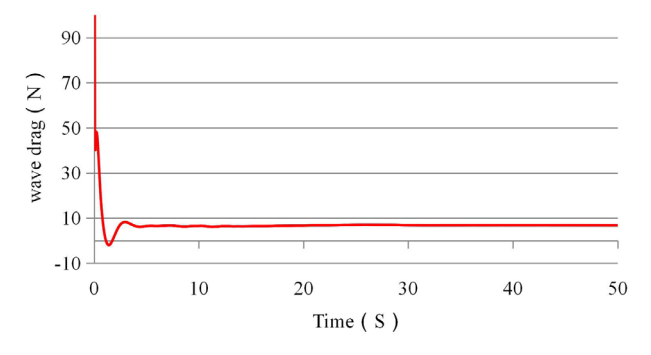
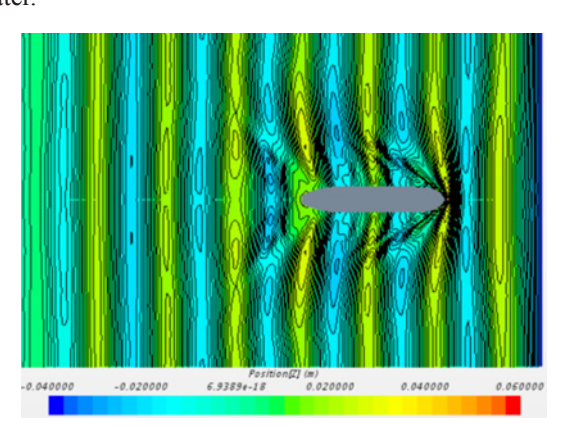
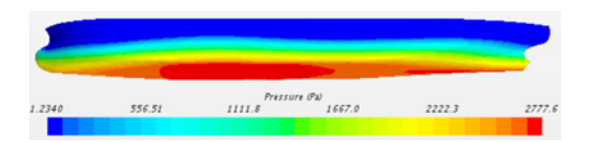


Figure 9. The resistance time history curve

Figure 10 shows the oscillogram of the free surface of the bare hull in waves. This oscillogram shows that the incoming current flows from the bow first, so the peak is formed at the bow. Near the middle of the ship, the change of the waveform is relatively stable. At the stern, a ship wave forms and gradually dissipates as the stern moves backward. It can be seen from the oscillogram that under the action of regular waves, the oscillogram of the free surface formed around the hull has slightly changed, which is not very different from the oscillogram in still water.



**Figure 10.** The oscillogram of the free surface of the bare hull in waves



**Figure 11.** The pressure profile of the free surface of the bare hull

According to Figure 11, the peak pressure appears near the bow and generally shows a decreasing-increasing-decreasing-increasing trend along the length of the boat. Among them, the pressure attenuates sharply at the bow and creates two low-pressure regions at the bow. Besides, this is the lowest pressure region of the entire hull in the waves. When it is close to the parallel middle body, it rises again. At the rear end of the parallel middle body near the stern, it first reduces the pressure value close to the parallel middle body. Then gradually increase along the stern. In general, speaking, the pressure distribution of the overall ship is not particularly noticeable.

#### 7. Resistance Calculation of Hull-propeller-rudder System

#### 7.1 Calculation Principle of Body Force Method

The VLM (Vortex Lattice Method), based on the potential flow theory, generates the body force that meets the requirements of the edge of the propeller blade [9]. It assigns the body force to the propeller's grid area, that is, it adds thrust and torque to replace the actual load on the surface of the propeller. The formula of the applied volume force source term is as follows:

$$F = \iiint_{\mathcal{X}} fbdV \tag{11}$$

$$fb_{x} = \frac{\rho U^{2}}{L_{pp}} A_{x} r^{*} \sqrt{1 - r^{*}}$$
 (12)

$$fb_{\theta} = \frac{\rho U^2}{L_{pp}} A_{\theta} \frac{r^* \sqrt{1 - r^*}}{(1 - Y_H)r^* + Y_H}$$
 (13)

Where, 
$$r^* = \frac{r_1 - R_H}{R_P - R_H}$$
,  $Y_H = \frac{R_H}{R_P}$ ,

$$A_x = \frac{C_t}{\Delta x} \cdot \frac{105}{(4 + 3Y_H)(1 - Y_H)}$$

$$A_{\theta} = \frac{K_{Q}}{J^{2} \Delta X} \frac{105}{\pi (4 + 3Y_{H})(1 - Y_{H})}$$

Where  $r_1$  represents the distance from any point in the propeller area to its axis;  $Y_H$  is the hub diameter ratio, that

is to say,  $R_P$  and  $R_H$  are the radii of the propeller and the radius of the hub, respectively; Ct is the dimensionless thrust coefficient;  $K_Q$  is the dimensionless torque coefficient.

#### 7.2 Modeling

The Body Force Method (BFM) is used to simulate the propeller. First, a virtual static disk model is created based on the specified propeller curve. The thrust coefficient Kt, torque coefficient KQ, process ratio J, and open water efficiency η are all derived from open water tests of the KVLCC1 ship's propeller in SIMMAN 2008. Secondly, determine the size and position of the virtual disk, and define the direction of the disk axis. Next, set the inflow velocity plane's properties. Make the velocity plane radius more significant than 10% of the virtual disk radius, and offset the velocity plane to 10% of the virtual disk diameter. Finally, set the virtual disk's rotation rate to be the rotation speed of the propeller in the open water test, which is 8.5rad/s. As shown in Figure 12.

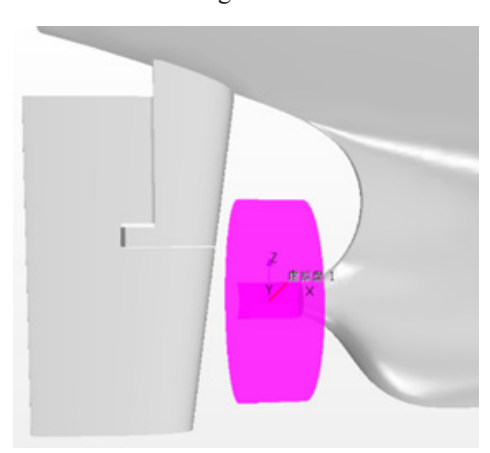


Figure 12. Propeller's action region

#### 7.3 Analysis of Calculation Results

Due to the large number of grids in the entire calculation, it takes about 40 hours in total to use an eight-core workstation. Comparing the results with the hydrostatic test. In Table 5, after considering the propeller rotation, the resistance of the ship-propeller-rudder system has increased by 13.49%. This shows that the propeller still has a significant influence on the hull resistance. Therefore, its

effect needs to be considered when calculating the actual resistance.

Figure 13 shows the oscillogram of the free surface of the ship-propeller-rudder system. From the oscillogram, the free surface presents a clear Kelvin wave, which reflects the reliability of the numerical simulation. The streamline diagram of the surface of the hull and rudder is shown in Figure 14. The streamline diagram shows that when the water flows through the propeller's action region, some streamlines are shifted because of the suction role of the propeller.

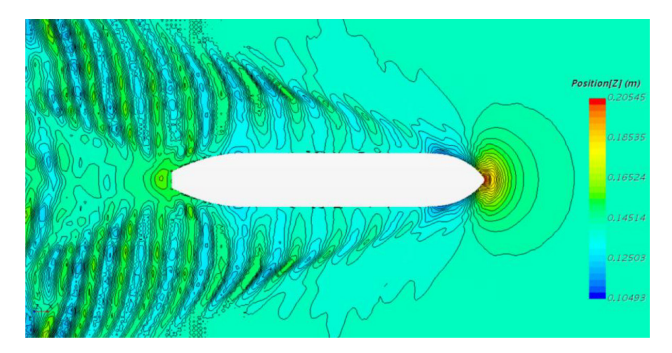


**Figure 13.** The oscillogram of the free surface of the ship-propeller-rudder system

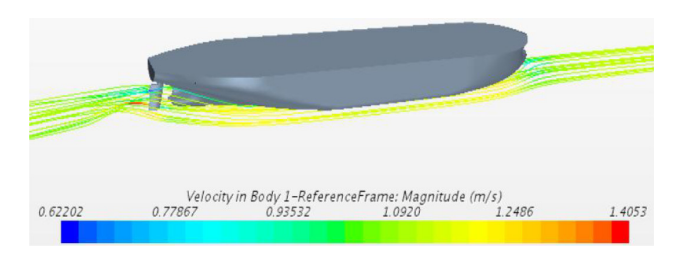


**Figure 14.** The streamline diagram of the surface of the hull and rudder

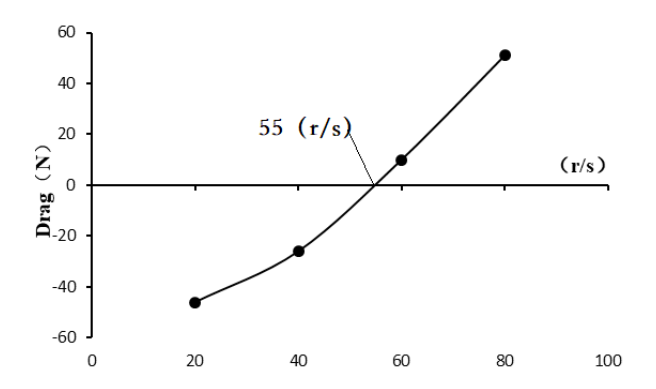
To further obtain the force condition of the ship-propeller-rudder system in the fluid, this paper sets four groups of different working conditions for calculation, Fr=0.142, as shown in Table 6. Analyze and use the data in Table 6 to draw Figure 15. It can be seen from the curve that the zero of the curves indicates that the net resistance is zero, which means that the resistance of the hull is balanced with the thrust generated by the propeller. If the shipping speed reaches 0.99m/s, the propeller's rotational speed needs to reach 55r/s.

Table 5. Comparison of resistance results (N)

Fn	Research object	Calculated value	Experimental value (Naked hull)	Deviation between the calculated value and experimental value
0.142	hull-propeller-rudder	36.84	31.87	13.49%

**Table 6.** The net resistance of the ship-propeller-rudder system (N)

Conditions	Rotational speed (r/s)	Propeller thrust	Resistance	Net resistance
1	20	5.5	-51.5	-46
2	40	24.5	-50.5	-26
3	60	59.5	-49.5	10
4	80	99.5	-48.5	51



**Figure 15.** The fitting curve of net resistance of the ship-propeller-rudder system

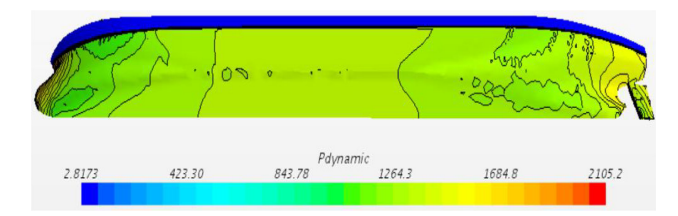


**Figure 16.** The pressure profile of the free surface of the ship-propeller-rudder system

Figure 16 shows the pressure distribution on the surface of the entire ship-propeller-rudder system during direct navigation. As shown from the pressure profile, since the rudder angle is not set, the hull surface pressure is symmetrical. There is a high-pressure area at the bow, mainly because it first contacts the inflow and forms a layered decrease along with the entire bulbous bow. Additionally, in the middle and front part, the shoulders on both sides of the hull and the bilge have a small range of low-pressure area, and the pressure in the entire parallel middle body is the same. The pressure at the rear end of the parallel midbody begins to decrease again until the pressure on the stern and the rudder's surface begins to increase gradually, and the pressure at the bottom edge of the rudder gradually decreases. This pressure change leads to the generation of vortices.

#### 8. Conclusion

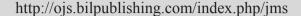
Based on the CFD theory, the calm water-resistance of the KLVCC1 ship was studied. Firstly, the reliability of the numerical simulation was verified by comparison with experimental values. Then the Stokes wave numerical wave tank was established to simulate the ship's resistance in waves. Finally, based on the body force model, the resistance of the ship-propeller-rudder system is studied. To sum up, the comparison with the static water experimental value proves that rudder and propeller's effect must be considered in the research of resistance through numerical simulation.

#### References

- [1] Ketut Suastika, Fajar Nugraha. Effects of Parallel-Middle-Body Relative Length and Stern Form on the Wake Fraction and Ship Resistance[J]. Applied Mechanics & Materials, 2017, 862: 278-283.
- [2] Andrea Farkas, Nastia Degiuli, Ivana Martić. Assessment of hydrodynamic characteristics of a full-scale ship at different draughts[J]. Ocean Engineering, 2018, 156: 135-152.
- [3] Yang Cai Hong, Han Duan Feng, Liu Feng. CFD numerical simulation of resistance prediction for large sea going ships[J]. Water transportation in China, 2017, 17(1): 80-81.
- [4] Du Yun Long, Chen Waei Min, Dong Guo Xiang. CFD calculation strategy of static water resistance of typical oil tanker model[J]. Journal of Jiangsu University of science and Technology (Natural Science), 2017, 31(5): 661-665.
- [5] Mingyu K, Olgun H, Osman T. Numerical studies on added resistance and motions of KVLCC2 in head seas for various ship speeds. Ocean Engineering, 2017, 140: 466-476.
- [6] Choi, Junwoo, Sung, Bum Yoon. Numerical simulations using momentum source wave-maker applied to RANS equation model[J]. Coastal Engineering, 2009, 56(10): 1043-1060.
- [7] Longo J, Stern F. Uncertainty Assessment for Towing Tank Tests with Example for Surface Combatant DTMB Model 5415. Journal Ship Research, 2005, 49(1): 55-68.
- [8] Jinbao Wang, Hai Yu, Yuefeng Zhang, et al. Numerical simulation of wake flow field and prediction of resistance performance for low speed and large ship[J]. Research and development of hydrodynamics, 2010, 25(5): 648-654.
- [9] Jeon M, Lee S, Lee S .Unsteady aerodynamics of offshore floating wind turbines in platform pitching motion using vortex lattice method. Renewable Energy, 2014, 65(5): 207-212.



#### **Journal of Marine Science**





#### ARTICLE

## An Evaluation of the Main Physical Features and Circulation Patterns in the Black Sea Basin

#### Alina Girleanu Eugen Rusu\*

"Dunarea de Jos" University of Galati, Faculty of Engineering, Mechanical Engineering Department, Galati, Romania

#### ARTICLE INFO

Article history

Received: 27 October 2020 Accepted: 18 November 2020 Published Online: 31 January 2021

Keywords:
Black Sea basin
Circulation patterns
Historical data
Climate change
Extreme values

#### ABSTRACT

Having as target the semi-enclosed basin of the Black Sea, the primary purpose of the existing paper is to present an overview of its extensive physical features and circulation patterns. To achieve this goal, more than five decades of data analysis - from 1960 to 2015 - were taken into consideration and the results were validated against acknowledged data, both from satellite data over the last two decades and in-situ measurements from first decades. The circulation of the Black Sea basin has been studied for almost 400 years since the Italian Count Luigi Marsigli first described the "two-layer" circulation through the Bosphorus Strait in the year 1681. Since climate change projections for the Black Sea region foresee a significant impact on the environment in the coming decades, a set of adaptation and mitigation measures is required. Therefore more research is needed. Nowadays, the warming trend adds a sense of immediate urgency because according to the National Oceanic and Atmospheric Administration's National Centre for Environmental Information, July 2020 was the second-hottest month ever recorded for the planet. Its averaged land and ocean surface temperature tied with July 2016 as the secondhighest for the month in the 141-year NOAA's global temperature dataset history, which dates back to 1880. It was 0.92°C above the 20th-century average of 15.8°C, with only 0.01°C less than the record extreme value measured in July of 2019.

#### 1. Introduction

The Black Sea is clearly one of the most conspicuous inland seas throughout the entire world. Squeezed between Central Asia and Western Europe, the wider Black Sea area borders Turkey to the South and Russia to the north. Following the Persian Gulf, this region is the second-largest reservoir of oil and natural gas and has considerable deposits of coal and, of course, a traditional adherence to fossil fuels [1]. At the same time, it is renowned for the

potential of its substantial renewable in hydropower, solar, and wind energy, and altogether [1-7], these factors raise awareness whenever climate change generate concern. The Black Sea is cut off from the world's ocean through its unique particularities. The dominant forces acting upon the Sea are represented by gravity, buoyancy - the floatation force of a material of lower density than the liquid that is immersed in - and wind, generating its dynamics of currents, tides, and mixing waters. Taking into consideration that the Black Sea's surface is relatively small

Eugen Rusu,

<sup>\*</sup>Corresponding Author:

<sup>&</sup>quot;Dunarea de Jos" University of Galati, Faculty of Engineering, Mechanical Engineering Department, Galati, Romania; Email: eugen.rusu@ugal.ro

- roughly 423 000 square kilometres - the surface tides produced by the gravitational attraction of the moon are almost insignificant. However, on the other hand, buoyancy maintains less dense layers of water floating on top of thicker ones, remaining unmixed, unless the buoyancy of either layer changes considerably through cooling of the lighter layers or warming of the denser ones. Another likelihood of mixing the layers would be the increasing or decreasing of the salt amount [8].

The Black Sea is permanently stratified, given the fact that it has developed two primary water layers which are separated by a strong density gradient, or pycnocline [8]. Its unique body of water is represented by the cold intermediate layer, below 70-150 metres, colder and saltier than the upper layer. It must be outlined that the Black Sea has a positive freshwater balance, which implies that it receives more freshwater from rivers (Europe's second, third, and fourth largest rivers - Danube, Dnipro, Don - flow into the Sea) and rainfall than it loses from evaporation [8]. Every year, the Black Sea receives roughly 350 square kilometres of river water and about 250 square kilometres of precipitation, while evaporation releases only 350 square kilometres of water [9]. Given the positive freshwater balance, the level of the Black Sea is higher than that of the Marmara Sea by an average of 0.43 metres [9]. Therefore, the excess of water flows through the Bosphorus Strait into the Marmara Sea, resulting in the development of two flows throughout the strait. The upper one leaves the Black Sea and transports surface water out of it.

Meanwhile, the bottom flow carries salty water, with salinity between 35 and 36% from the Mediterranean to the Black Sea <sup>[9]</sup>. The much saltier water mixes with the waters of the basin, ending in a relatively low salinity at the surface, with an average of 18.2%, though it could be much lower near river outflows. The lower layer of the Bosphorus Strait has an average salinity of 21.8%. One could say that a difference of 3.6% is insignificant, but is enough to prevent the bottom, hydrogen sulfide water from reaching the sea surface <sup>[4,8]</sup>, posing a significant threat to human life and the surrounding environment <sup>[8]</sup>.

According to statistics and researchers [8-10], an average of 300 cubic kilometres of bottom water mixes into the surface layer yearly, which is equivalent to a layer of almost 2 millimetres thick of bottom water per day. Therefore, it would take somewhere near 2000 years for all that bottom water to be circulated through the pycnocline [8]. According to [8], the layer nearest the surface with constant density is mixed by the wind and waves, and it is known as the "upper mixed layer". Secondly, the deepwater area has minimal variation regarding the density, and the

temperature is warming the water near the surface - the measurements took place during middle spring - but it is getting colder with depth until a cold intermediate layer of around 7.5-8°C is reached. The more bottomless Sea is warmer, mainly from the Mediterranean water, but also from geothermal processes underneath the seabed [8].

Gradually, but at a plodding pace, the bottom water layer does mix, to form the upper layer. The rate of overall mixing can be determined from the water balance through the Bosphorus Strait, as it is the only gateway of seawater to the Black Sea. Logically, in the long run, the amount of salt entering must be equal to the one leaving; otherwise, the seawater would become fresher or saltier [8].

#### 2. Circulation Patterns in the Black Sea Basin

On a global scale, thermohaline circulation is part of the ocean circulation driven by density gradients created by surface heat and fluxes of freshwater, and it is a significant regulator of the Earth's climate. The thermohaline circulation process of the Black Sea is similar but on a smaller, regional scale. One of the distinctive characteristics of the Black Sea is the cold intermediate layer (also known as CIL), a relic of the cold winter water masses, which in summer are covered by warmer surface water, being a subject of constant debate among researchers. Different hypotheses on the establishment of the cold intermediate layer were put forward throughout the years. Some say that it was formed as a result of advective and convective contributions taking place along anticyclonic regions of the Sea, largely dawning from the shelf and the continental slope area throughout the winter and expanding during spring and summer [11]. It was Luigi Marsigli who first recognized that the Bosporus currents were purely a simple outcome of the difference among the water densities in the Black and Mediterranean Seas. He succeeded in demonstrating this density difference by developing a physical model that captured the striking features of the phenomenon that has intrigued oceanographers since 1681 - considered by scientists the year of the foundation of modern oceanography [12]. Water from the cold intermediate layer is essential for the biology of the Black Sea since it is richer in plant nutrients than offshore surface water and fertilizes the Sea when it is mixed back to the surface [8].

The Black Sea's general circulation features consist mainly of the cyclonic Rim current, drifting along the continental slope, and various cyclonic and anticyclonic mesoscale eddies located inside the primary current or between it and the shore [4,13]. Nevertheless, the mesoscale eddies emerge along the borderline of the basin, as part of the Rim structure. It is mesoscale circulation that ef-

fectively links coastal hydrodynamic and geochemical processes to those in the deep Sea, hence providing a mechanism for two - way transport between nearshore and offshore areas [13].

Horizontal circulation of the Black Sea is characterized by gyres, which are wind-driven cyclonic and anticyclonic currents with similar dimensions to that of ocean basins. Black Sea's circulation is nearly driven by the winds and the buoyancy differences between inflowing freshwater and the saltier Mediterranean inflow [8]. Consequently, throughout the year there is a cyclonic circulation at variable speed. Figure 1 depicts a changeless feature of the upper layer circulation - the Rim Current surrounding the whole Black Sea. From place to place, it has a width of some tens of kilometres and sometimes may achieve a maximum speed of 0.8-1 knot, which is between 40 and

50 cm/sec, at times increasing up to 1.6 knots, or 80-100 cm/sec <sup>[8]</sup>. Direct observations have determined these results and in situ measurements, as well as available satellite data of the current velocity from surface buoys <sup>[8,11,14]</sup>. Figure 1 reveals the circulation of the Black Sea on 23<sup>rd</sup> of October 2020 using a snapshot from <sup>[14]</sup>, and the navigation traffic at that specific moment.

Figure 2 indicates the characteristics of the circulation in gyres, with the permanent Rim current following the continental shelf, as a general rule. Nevertheless, the coast's shape sends it on seawards short cuts in some places, outwitting another gyre, much smaller, between the coast and the Rim - Bosphorus gyre, in the south-western part, and the Batumi gyre, in the south-eastern coast, both of them represented as continuing features. Inside the Rim current, there are two (more or less) permanent gyres,

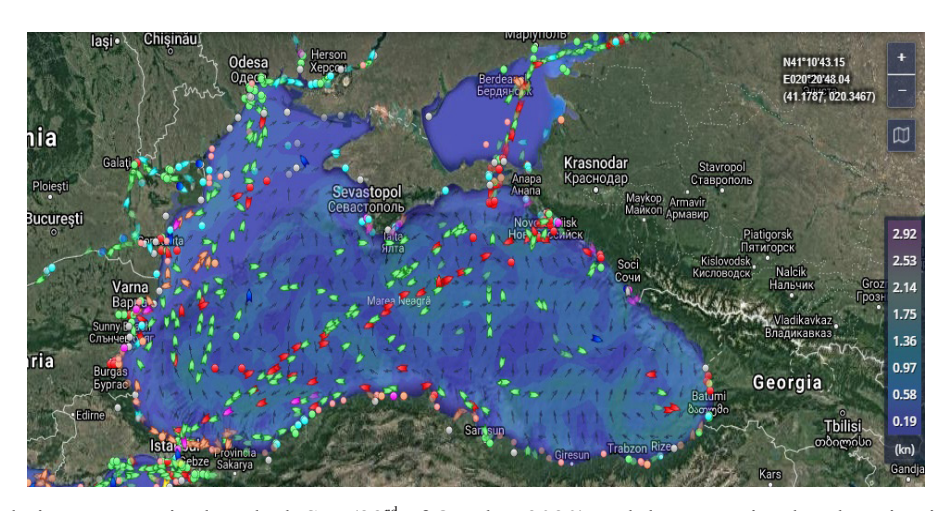


**Figure 1.** Circulation patterns in the Black Sea (23<sup>rd</sup> of October 2020) and the most circulated navigation routes. Snapshot from [14]

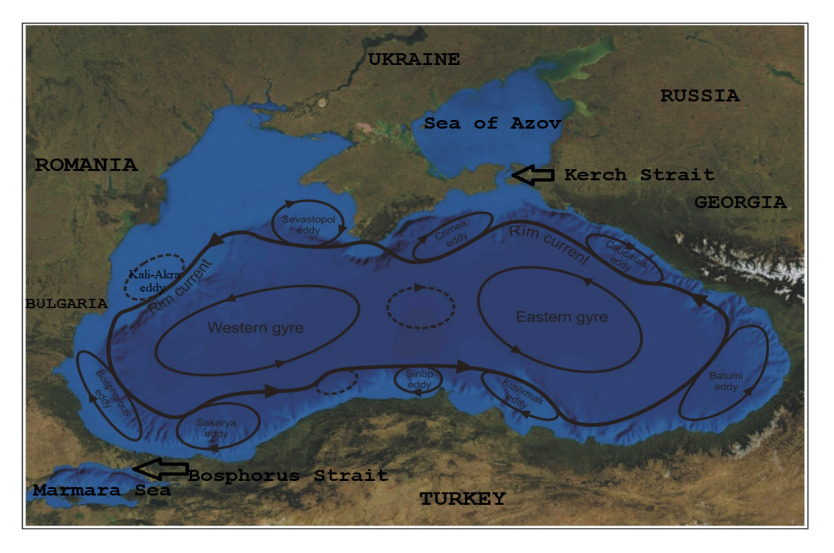


**Figure 2.** Schematic diagram of the general circulation in the Black Sea basin - the solid lines indicate the habitual features of the general circulation. (Modified satellite map provided by NASA - a screenshot from NASA's globe software World Wind)

marked and known as the "Western" and "Eastern" gyres. They are of great significance as they mark the pathway of planktonic larvae - that cannot swim against the currents and their whole lifecycle has been adjusted to the circulation. Within the Rim Current and the shore, there is also a range of seasonal gyres, with as much significance as the ones as mentioned earlier, as they play a significant role in the redistribution of Danube and Dnipro's water and mixing it with the Black Sea surface water [8].

It has been confirmed that the interannual wind variability has a meaningful effect on the mesoscale activity and consequently on the Black Sea's circulation. The mesoscale activity is shallow when the wind force has long-lasting, vital cyclonic events which strengthen the large scale circulation. However, the large scale circulation is less intense, and the mesoscale activity expands when the wind is anticyclonic. Consequently, it is of utmost importance to take into consideration wind variability in numerical modelling to avoid undervaluing the contribution of critical physical processes that dominate the ocean's response to the climatic forcing, as presented in [11,15,16].

Knipovich first described in 1932 that the general cyclonic circulation is attributed to the cyclonic nature of the wind field. Nevertheless, various classifications and further investigation of the circulation have been carried out since then, suggesting that the circulation patterns are dominated by fundamental factors such as the sequence of the seasonal thermohaline circulation induced by non-uniform surface fluxes, the wind, and the topography of the basin. Another major determinant that contributes to the Black Sea's general circulation is the freshwater inflow from the rivers along with the dense Mediterranean inflow in the Bosphorus proximity, generating lateral buoyancy fluxes. The spatiotemporal inconstant sub-basin scale features are typically cyclonic gyres in the deep Black Sea and some anticyclones positioned at the shelf split between the coast and the Rim Current.

The semi-permanent characteristics are schematized in figure 2. Beginning from the north-eastern part, in a clockwise way, the Caucasus eddy in the north-eastern coast, the Batumi eddy in the south-eastern corner of the basin, a range of anticyclones along the Anatolian coast (including the Sakarya, Sinop and Kizilirmak eddies), the Bosphorus and Kali-Akra eddies in the western part, the Sevastopol eddy at the west of the Crimean peninsula, and the Crimea eddy at the east of the peninsula.

Generally, seas have a significant component of mesoscale circulation [11], and eddying movements are nearly everywhere. Eddies stir the flow, transport heat and trace chemicals across it. Globally, the humblest circulations are

merely a few millimetres in size, yet the greatest is more than ten thousand kilometres in diameter. Circumstances such as latitude, nearby bottom topography, energy level, as well as the nature of their generation, contribute to the variation of the horizontal scales of mesoscale eddies [11]. This fabulous range of variety comes from the tendency for the high-latitude ocean to have lighter density stratification and larger Coriolis rate. Mesoscale eddies are often created by the uncertain meandering of a strong current where the waving deflection of the current is itself a form of the underlying eddy, which might finally turn into a circular one. However, wind or a colder sea surface water, as well as a flow over a former island or rocky seafloor can contribute to the creation of a mesoscale eddy, which is a fundamental mechanism of transport of impulse, heat, and trace water properties (for example oxygen, chemicals, biological communities, and nutrients).

As regards the Black Sea, oceanographic surveys and the availability of satellite data added considerable detail to the description of its circulation. Thus, a novel feature discovered is that the regular circulation is not as steady as beforehand thought, and there is unusual mesoscale activity in the region. While mesoscale eddies in the Black Sea usually have 80 to 100 kilometres in diameter and they seep deeply into the pycnocline (dropping to almost 400 m in some areas), with a velocity near the sea surface between 15 and 50 cm/s.

#### 3. Statistical Analysis of the Circulation Patterns in the Black Sea Basin Using Satellite Data, Recent Measurements, and Simulations with Numerical Models

It has been stated that the general circulation of the Black Sea is wind-driven and also driven by extensive freshwater input from the "three-D" rivers - Danube, Dnipro, and Don. In the year 1994, the Danube river was declared one of the ten Pan-European transport passageways - the seventh one. The Danube outflow produces a current system that seldom generates strong interactions with waves - especially at the Saint George's arm in the southern part [2]. Its alluvium has led to the creation of the Sacalin Islands in 1897, which measure 19 kilometres in length - and still growing.

Generally speaking, validated models that have been used to reproduce the Black Sea hydrodynamics fall into two major categories, such as data assimilation models and those with weak/strong relaxation. An approach of the interannual variability of the Black Sea's hydrodynamics is reported in [17], providing a model without relaxation; however, neither sea surface salinity nor water column

salinity is displayed. The models presented in [18,19,20,21] are based on data assimilation and available satellite data for altimetry and sea surface temperature to force model works. Given the lack of consistent data for sea surface salinity, typically climatological datasets are utilized instead. However, they failed to replicate the vertical Black Sea thermohaline structure, such as the cold intermediate layer's properties, realistically, but are suitable for operational forecasting (CMEMS, [4]). The second category includes stand - alone ocean models with distinct relaxation plots to climatological or observational sea surface temperature and sea surface salinity time series.

Because of the complexity and hardness of reproducing the surface salinity and its extensive vertical gradients, newer versions of statistical modelling of currents are bound to continue to use sea surface salinity relaxation. Besides, the Black Sea's surface salinity observational data is still rare and meagre. Notwithstanding its shortcomings, the present data can be used to some extent for relaxation in hindcast simulations, as presented in [19,20,21]. Nevertheless, a model capable of performing scenarios for the future is highly needed, not only for the phytoplankton blossom but also to foresee potential ecological changes.

Consequently, these factors motivated researchers to generate a model capable of simulating the mesoscale and thermohaline circulation in the Black Sea for a perpetual multidecadal period without any relaxation via external fields. The 3D hydrodynamic model presented in [13] covers the 3D General Estuarine Transport Model (known as GETM - which implements primitive equations with hydrostatic approximations to calculate the 3D flow field and the free surface [22]) and the General Ocean Turbulence Model (known as GOTM). The goal of the scientists was The study presented in [23] emphasizes the realistic representation of the Black Sea circulation and mean thermohaline structure, with a particular focus on the mean sea surface salinity variation. Since salinity, temperature and density are approximately uniform in the deep water, the main focus is on the dynamics of the upper surface down to 250 metres depth. Besides, long - term trends of temperature over salinity fluctuations are discussed.

Having as target the Black Sea basin, the increased resolution obtained from oceanographic surveys and the availability of satellite data (AVISO - Archiving, Validation, and Interpretation of Satellite Oceanographic data and ECMWF - European Centre for Medium-Range Weather Forecasts) added considerable detail to the description of its circulation. Thus 18 years of satellite data were analyzed from 1993 until 2010<sup>[5]</sup> to achieve a greater level of understanding of the circulation in the Black Sea basin. The satellite data was obtained from AVISO and contained daily measurements of the "U-V" parameters of the currents with a spatial resolution of roughly 10 kilometres horizontally and 13 kilometres vertically. The monthly averaged values of the current velocity are pre-

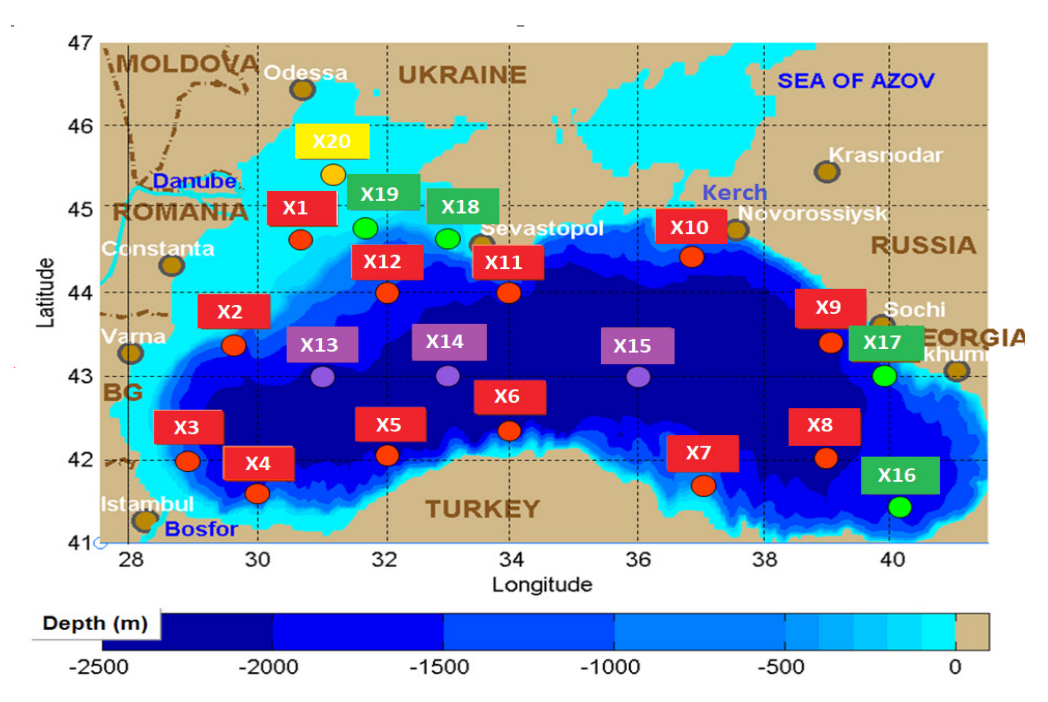


**Figure 3.** The bathymetry of the Black Sea (from GEBCO - The General Bathymetric Chart of the Oceans) with 20 points of reference

**Table 1.** Monthly averaged values of the current velocity (measured in ms<sup>-1</sup>) for the reference points taken into consideration [X1 - X20] for 18 years, from 1993 until 2010

<b>S</b> . ( ( ) ( ) ( ) ( ) ( )						Months						
Points (with coordinates)	January	February	March	April	May	June	July	August	Sep.	Oct.	Nov.	Dec.
X1(44.4N/30.43E)	0.08	0.07	0.07	0.08	0.08	0.07	0.07	0.06	0.06	0.06	0.06	0.07
X2 (43.18N/29.43E)	0.11	0.12	0.13	0.12	0.11	0.11	0.09	0.11	0.11	0.10	0.10	0.11
X3 (41.58N/29E)	0.13	0.12	0.13	0.11	0.10	0.09	0.11	0.12	0.11	0.10	0.11	0.10
X4 (41.36N/29.58E)	0.08	0.08	0.08	0.09	0.07	0.07	0.07	0.08	0.09	0.08	0.08	0.09
X5 (42.7N/31.59E)	0.06	0.06	0.06	0.07	0.07	0.06	0.06	0.05	0.06	0.08	0.08	0.07
X6 (42.21N/34.2E)	0.08	0.08	0.08	0.07	0.08	0.07	0.07	0.08	0.07	0.07	0.07	0.07
X7 (41.32N/36.59E)	0.07	0.09	0.08	0.08	0.06	0.06	0.07	0.07	0.08	0.08	0.08	0.08
X8 (42.1N/39.3E)	0.14	0.10	0.10	0.10	0.09	0.11	0.12	0.13	0.13	0.11	0.12	0.13
X9 (43.32N/39.14E)	0.13	0.11	0.11	0.11	0.11	0.10	0.10	0.13	0.12	0.11	0.13	0.12
X10(44.38N/36.49E)	0.15	0.14	0.14	0.13	0.10	0.11	0.13	0.13	0.15	0.15	0.13	0.14
X11 (43.59/33.59E)	0.08	0.07	0.07	0.07	0.07	0.07	0.06	0.06	0.08	0.08	0.08	0.07
X12 (44N/32E)	0.15	0.14	0.16	0.18	0.17	0.16	0.15	0.13	0.13	0.14	0.12	0.14
X13 (43N/30.6E)	0.07	0.09	0.08	0.08	0.08	0.08	0.07	0.07	0.08	0.09	0.10	0.08
X14 (43.1N/32.58E)	0.07	0.06	0.07	0.07	0.06	0.07	0.06	0.07	0.06	0.07	0.07	0.07
X15 (42.59N/36E)	0.08	0.08	0.08	0.08	0.07	0.08	0.09	0.09	0.09	0.10	0.09	0.08
X16 (41.23N/40.4E)	0.11	0.10	0.11	0.10	0.11	0.12	0.11	0.10	0.11	0.11	0.10	0.11
X17(43.32N/9.57E)	0.12	0.08	0.09	0.09	0.10	0.09	0.09	0.09	0.11	0.14	0.14	0.13
X18 (44.37N/33E)	0.11	0.12	0.12	0.10	0.10	0.10	0.10	0.09	0.12	0.12	0.10	0.12
X19 (44.4N/31.46E)	0.18	0.18	0.18	0.17	0.16	0.18	0.17	0.14	0.14	0.13	0.14	0.16
X20 (45.21N/31E)	0.07	0.07	0.07	0.06	0.06	0.06	0.06	0.07	0.07	0.08	0.08	0.07

sented below in table 1, with results provided by AVISO. The 20 points of reference taken into consideration are outlined in figure 3, having the bathymetric map of the Black Sea in the background.

At first glance, the values outlined in table 1 confirms that the average current velocity values in the Black Sea basin are normally low, compared to the Global Ocean. Most of the points selected on the Rim cyclonic current and at the edge of the anticyclonic eddies have higher velocities than the ones located in the north-western shelf and central gyres. Another characteristic of the Black Sea's current velocities is the variation between summer and winter periods, as the table reveals that the lowest

values are measured during June, July, and August. The points in the interval [X1-X12] have higher current velocities, being positioned near the Rim current. The points with almost insignificant velocity variation are those in the interim determined by [X1 - X6], points positioned in the south-western part of the Black Sea. In addition, the points situated on the Rim or the two anticyclonic eddies have greater velocity values than, for example, X13, X14 and X15, points located inside the Rim current. As regards point X20, which is situated in the north-western shelf, it can be observed that it has the smallest value and no other significant circulation feature can be recognized.

#### 4. Discussion

According to the National Oceanic and Atmospheric Administration's National Centre for Environmental Information, July 2020 was the second-hottest month ever recorded worldwide. Its averaged land and ocean surface temperature tied with July 2016 as the second-highest for the month in the 141-year NOAA's global temperature dataset record, which dates back to 1880 [24]. It was 0.92°C above the 20th-century average of 15.8°C, with only 0.01°C less than the record extreme value measured in July of 2019. From a regional point of view, warmer winters are beginning to remould the structure of the Black Sea, which could foreshadow how ocean configurations might vary from future climate change, according to brand-new observations and research [25].

Studies imply that what is causing the CIL to warm is climate change, as gigantic water masses determine the planet's climate and transfer nutrients throughout the world. Therefore, changes in oceanic masses' composition might remodel global currents, with adverse effects on the global ecosystems. Since it is quite challenging to study massive masses of water as a whole, researchers and oceanographers use regional water masses to discover how oceanic masses could be affected [25]. A novel study published last year in American Geophysical Union's Journal of Geophysical Research-Oceans and analyses salinity, density, and seasonal temperatures in the Black Sea during the last 14 years reveals a warming trend in the middle layer of the Black Sea (CIL). As has been outlined in other publications [13,16,23,26-29], this unique layer had its fluctuations in the past, but since 2005 its core temperature has warmed up to 0.7 °C, according to [25]. The blending of the other layers of water with the CIL will, consequently, allow the masses of water from the deeper layers of the Sea to infiltrate into the surface one. Thus hazardous impacts on the marine environment might befall, and it could even lead to the displacement of hundreds of millions of inhabitants from the coastal area.

Due to its specific and unique thermohaline structure, the Black Sea is of keen interest. A warming trend in the surface water is not precisely defined for the last century, while a positive trend for the last three decades has been demonstrated in [23,26]. Consequently, changes in the regional climate appear to have their impact firstly on other thermohaline features, such as the temperature of intermediate layers, succeeded by an increase in the temperature of the sea surface water. The CIL, whose formation and evolution are not yet entirely explained, it is certain to

have the lowest Black Sea temperature - less than eight °C - and most of its pycnocline [27-29]. Since in the Black Sea basin has been meaningful ecological degradation since the 1970s, mainly due to overfishing, pollution and natural climatic changes. To understand at least up to a certain extent how the Black Sea's circulation and physical features may evolve in the near future, simulations of future scenarios and mapping courses in its ecosystem are a matter of immediate urgency.

There have been numerous studies and significant research related to the Black Sea's cold intermediate layer and its general circulation patterns [31-37], but little information has been presented on its changes over time. In this up-to-date study [25], researchers mapped the evolution of the Black Sea's CIL in the period from 2005 until 2019, comparing its development with the region's climate courses. Utilizing battery-powered buoys to measure salinity, density, and temperature from the sea surface down to one thousand metres, at various points throughout the year. Thenceforth, after comparing the measurements with the surface air temperature in order to find a correlation between the weather and the CIL's salinity and temperature, the result was that weather fluctuations during wintertime changed the temperature and salinity of the CIL while keeping the density values almost the same.

The trials performed in <sup>[23]</sup> comprising more than 50 years of data analysis revealed no major long-term trend in the Sea's average surface water temperature. This absence of a trend is a fundamental discovery based on a long-term trial that had not previously been fortunately conducted. This period from 1960 to 2015 was taken into consideration, and the results provided were compared with acknowledged data from available satellite data over the last two decades and less complete, but reliable data, from first decades. Before the accomplishment of this study <sup>[23]</sup>, experts had relied on scarce surface temperature values from ship cruises to understand the Black Sea's particular features better.

The final results of the simulation presented in figure 4 came as a great astonishment to researchers. They expected the study to reveal some warming trend, while it revealed a decreasing course in salinity at the surface of the Black Sea of 0.02% per year. There was no particular correspondence between wind speed or direction and salinity, which implies that combinations of weather contingencies are accountable for this trend.

Furthermore, three distinct periods outlined an important shift in the saltwater and temperature properties of the Sea, and these are between 1960 and 1970, 1970 and

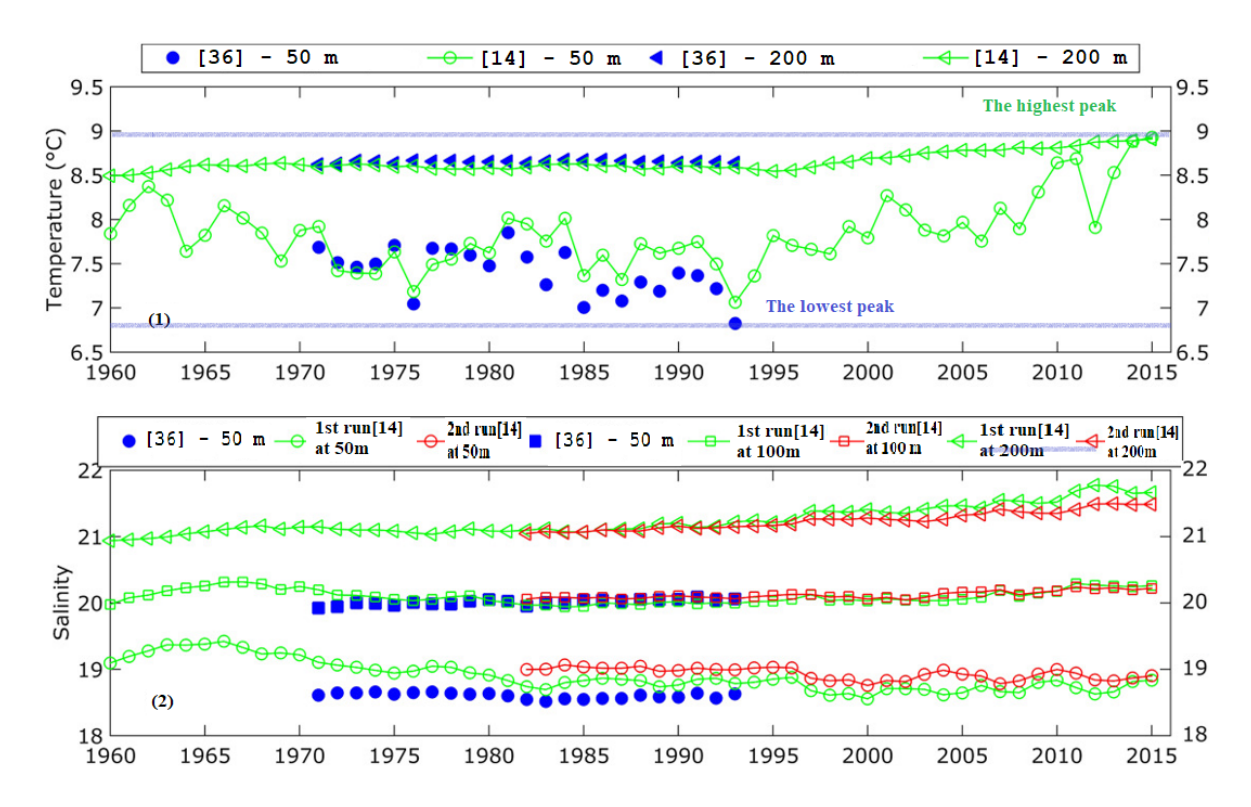


**Figure 4.** Time series from observations and simulations: (1) averaged temperature over the interior basin at levels of 50 metres, and 200 metres depth; (2) salinity averaged over the Black Sea basin at levels of 50, 100, and 200 metres depth from the first and second run—reanalysis data processed from [23] and [36]

1995, and 1995 to 2015. This observation may be related to the changes of currents that took place in the Sea's general circulation, as these periods were characterized by major changes from a small and disorganized current circulation during 1960 until 1970, to a strong central Rim circulation starting from 1970 until 2015, as outlined in [23].

Even though there has been no long-term positive trend in the temperatures measured at the surface waters of the Black Sea, this does not mean that it is "untouched" by the global warming trend. One explanation might be that air temperature in the region is still increasing, thus hiding or moderating these effects. The study [23] even took into account the average temperature trends at particular depths (50, respectively 200 metres), resulting in a positive course at 50 metres below the surface, which implies a warming pattern of the deeper waters, instead of the surface layer.

Moreover, the study confirmed that the surface waters are colder in the central-deep interior parts of the Black Sea basin during winter, as well as the moving of cold water masses formed in winter on the north-western slope by the principal cyclonic current and by mesoscale eddies

on the shelf break <sup>[38,39]</sup>. The innovative part of the study is the quantification of the significance of these newest findings during an extended period. Particularly, the fact that surface waters are colder than usual play a crucial role in the cold intermediate layer's formation in the interior basin, while the transport of cold water masses regulates the renewal of the cold intermediate layer along with the principal cyclonic currents and the exterior basin, also in the south-eastern part of the basin <sup>[23]</sup>.

To completely isolate the effects of basin circulation and the contribution of the north-western shelf cold water masses, the Joint Research Centre studied the frequency of a latent tracer originating in this area. The result shows that a substantial fraction of the cold north-western shelf water mass is transported through the principal cyclonic current to the eastern confluence and anticyclonic regions. In contrast, only a tinier fraction of the cold water mass is transported to the central part of the basin. The temporal cooling capacity of the cold intermediate layer is extremely variable and has decreased dramatically during the past decade, being comparable to nothing, which insinuates that the CIL has disappeared, as figure 5 outlines.

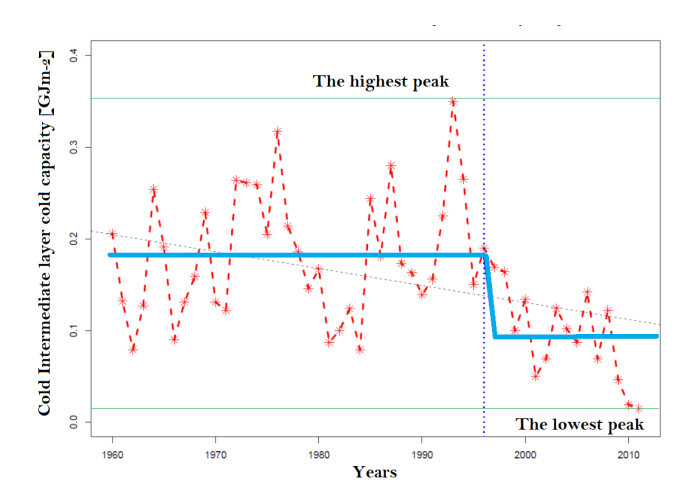


**Figure 5.** The CIL cold capacity trend is showing a dramatic drop at the beginning of the 21 st century

Therefore, the additional heat from regional warming is transported downward to greater depths, thus warming the CIL, instead of contributing to the warming of the upper layer. This could potentially explain the missing increasing temperature trend in the Black Sea surface waters reported in 2019 by the European Commission of Science [30].

#### 5. Conclusion

A first conclusion that can be drawn is that in most of the cases a good correlation between the satellite data, historical data, and simulation results can be observed, revealing a warming trend during the last decades. Should this warmer trend happen to continue, there might be potential changes in the stratification of the unique Black Sea, that could carry sulfide, noxious and corrosive chemicals from the bottom of the Black Sea, up to the upper surface layer, endangering aquatic wildlife and tourism as well. Even though past research has proved that the Black Sea's water layers had their cycles through warm and cold times since the 1950s, the CIL has never touched this extraordinary temperature. Nevertheless, more intensive analysis on the progression of the Black Sea's circulation must be conducted, along with studies on the cold intermediate layer and its fluctuations, to determine whether global warming is responsible for the cold intermediate layer's gradual disappearance or not.

Physical oceanography is a fascinating and complex study, and as it has been proved in this paper, the chemistry and the biology of the Sea are in direct correlation with the physical processes within it. The state-of-the-art satellite measurements are improving our understanding of physical processes. Knowledge of the main physical features and circulation patterns in the Black Sea is of paramount importance, as their trends and variability might

pose a significant threat to an extensive range of marine pursuits. Such activities might include a safe and economical design and development of offshore oil and gas amenities, naval architecture design, decisive planning for extended marine towing operations. Additionally, a better understanding of the wind, wave and the current climate is indispensable for coastal foundation, including lessening shoreline erosion and more extensive protection, sediment transport and wave search for seafloor pipeline, as well as a better design of harbours.

Overwhelming is the fact that scientists warn that if the global average temperature rises by another three °C, sea and ocean levels will rise by approximately 6.5 meters. Such apocalyptic scenarios will lead to the displacement of hundreds of millions of people from the coastal region, including the Black Sea coast. Moreover, the average temperature of the Earth's surface has already risen by one degree since the end of the 19<sup>th</sup> century, enough to lead to extreme weather events. However, an increase from 2 to 6°C can lead to a real catastrophe. Climate change would destroy civilization and redraw the map of the world. From 6°C upwards, sea and ocean levels would rise by 10 meters for each degree, which would raise the oceans to levels not seen for millions of years.

#### Acknowledgments

This work was carried out in the framework of the research project DREAM (Dynamics of the REsources and technological Advance in harvesting Marine renewable energy), supported by the Romanian Executive Agency for Higher Education, Research, Development and Innovation Funding - UEFISCDI, grant number PN-III-P4-ID-PCE-2020-0008.

#### References

- [1] Gîrleanu, A., Rusu, E. Evaluating and Preventing Pollution From Navigation in the Black Sea Coastal Areas in the Context of Climate Change, Mechanical Testing, and Diagnosis, 2019, 9(4): 19-24. Available at:
  - https://search.proquest.com/docview/2431837409? accountid=17242
- [2] Rusu, E. Modelling of wave-current interactions at the mouths of the Danube, Journal of Marine Science and Technology, 2010, 15(2): 143-159.

#### DOI: 10.1007/s00773-009-0078-x

[3] Kara, A. B., Wallcraft, A. J., Hurlburt, H. E. A new solar radiation penetration scheme for use in ocean mixed layer studies: An application to the Black Sea using a fine - resolution Hybrid Coordinate Ocean Model (HYCOM), J. Phys. Oceanogr., 2005, 35: 1332.

#### DOI: 10.1175/JPO2677.1

- [4] Rusu, E. Strategies in using numerical wave models in ocean/coastal applications, Journal of Marine Science and Technology, 2011, 19(1): 58-75.
- [5] Toderascu, R., Rusu, E. Evaluation of the Circulation Patterns in the Black Sea Using Remotely Sensed and in-situ Measurements, International Journal of Geosciences, 2013, 04(07): 1009-1017.

#### DOI: 10.4236/ijg.2013.47094

[6] Toderascu, R., Rusu, E. Implementation of a Joint System for Waves and Currents in the Black Sea, International Journal of Ocean System Engineering, 2014, 4(1): 29-42,

#### DOI: 10.5574/ijose.2014.4.1.029

- [7] Rusu, E., Onea, F., Toderascu, R. Dynamics of the environmental matrix in the Black Sea as reflected by recent measurements and simulations with numerical models, The Black Sea: Dynamics, Ecology and Conservation, 2011.
- [8] Black Sea Study Pack. A resource for teachers, edited by Laurence Mee, Olga Maiboroda, the Black Sea Ecosystem Recovery Project, Istanbul, Turkey, 2006.
- [9] http://blackseascene.net (accessed on 23.10.2020).
- [10] State of the Environment of the Black Sea (2001 2006/7), edited by Temel Oguz. Publications of the Commission on the Protection of the Black Sea Against Pollution (BSC) 2008-3, Istanbul, Turkey: 448.

#### ISBN: 978-9944-245-33-3

- [11] Ortiz, E., Elizabeth, C. Mesoscale circulation in the Black Sea: a study combining numerical modelling and observations, 2005.
- [12] Soffientino, B., MEQ. Pilson. The Bosporus Strait: A special place in the history of oceanography, Oceanography, 2005, 18(2):16-23. https://doi.org/10.5670/oceanog.2005.38
- [13] Miladinova, S., Stips, A., Garcia-Gorriz, E. Black Sea thermohaline properties: Long-term trends and variations, J. Geophys. Res. Oceans, 2017: 5624-5644.

#### DOI: 10.1002/2016JC012644

- [14] https://www.marinetraffic.com (accessed on 27.10.2020)
- [15] Markov, A. A. et al. Circulation in the surface and intermediate layers of the Black Sea, 1992.
- [16] Oguz, T., Latun, V., Latif, M., Vladimirov, V. Circulation in the surface and intermediate layers in the Black Sea, 1993: 1597-1612.
- [17] Capet, A., Barth, A., Beckers, J. M., Grégoire, M. Interannual variability of Black Sea's hydrodynamics and connection to atmospheric patterns, Deep-Sea

Res., Part II, 2012: 77-80+128-142.

#### DOI:10.1016/j.dsr2.2012.04.010

[18] Bai, J., P. Perron. Computation and Analysis of multiple structural change models, J. Appl. Econ., 2003, 18: 1-22.

#### DOI: 10.1002/jae.659

[19] Korotaev, G., Oguz, T., Nikiforov, A., Koblinsky, C. Seasonal, interannual, and mesoscale variability of the Black Sea upper layer circulation derived from altimeter data, J. Geophys. Res., 2003, 108(C4): 3122.

#### DOI: 10.1029/2002JC001508

[20] Dorofeev, V. L., Korotaev, G. K., Sukhikh, L. I. Study of long - term variations in the Black Sea fields using an interdisciplinary physical and biogeochemical model, Izv. Atmos. Oceanic Phys., 2013, 49(6): 622-631.

#### DOI: 10.1134/S0001433813060054

[21] Dorofeev, V. L., Sukhikh, L. I. Analysis of variability of the Black Sea hydrophysical fields in 1993-2012 based on the reanalysis results, Phys. Oceanogr., 2016, 1: 33-47.

#### DOI: 10.22449/1573-160X-2016-1-33-47

- [22] https://www.noaa.gov (accessed on 27.10.2020).
- [23] Miladinova, S., Stips, A., Garcia-Gorriz, E. Black Sea thermohaline properties: Long-term trends and variations, J. Geophys. Res. Oceans, 2017: 5624-5644.

#### DOI: 10.1002/2016JC012644

[24] Stanev, Emil V., et al. Climate Change and Regional Ocean Water Mass Disappearance: Case of the Black Sea, Journal of Geophysical Research: Oceans, DOI. org (Crossref), 2019.

#### DOI: 10.1029/2019JC015076

[25] Stanev, Emil V., et al. Climate Change and Regional Ocean Water Mass Disappearance: Case of the Black Sea, Journal of Geophysical Research: Oceans, DOI. org (Crossref), 2019.

#### DOI: 10.1029/2019JC015076

[26] Miladinova, S., Stips, A., Moy, D. M. Progress in Oceanography Formation and changes of the Black Sea cold intermediate layer, Progress in Oceanography, 2018, 167(May): 11-23,

#### DOI: 10.1016/j.pocean.2018.07.002

- [27] Filippov, D.M. Water circulation and structure of the Black Sea, Nauka, Moscow, (in Russian), 1968: 136
- [28] Oguz, T., Besiktepe, S. Observations on the Rim Current structure, CIW formation and transport in the Western Black Sea, 1999: 1733-1753.
- [29] Ovchinnikov, I.M., Popov, Yu.I. Formation of a cold intermediate layer in the Black Sea, Oceanology, 1987: 555-560.

- [30] https://europa.eu/ (accessed on 29.10.2020).
- [31] Stanev, E. V., Roussenov, V. M., Rachev, N. H., Staneva, J. V. Sea response to atmospheric variability: Model study for the Black Sea, J. Mar. Syst., 1995, 6: 241-267.

#### DOI: 10.1016/0924-7963(94)00026-8

- [32] Stanev, E. V., Beckers, J. M. Barotropic and baroclinic oscillations in strongly stratified ocean basins: Numerical study of the Black Sea, J. Mar. Syst., 1999, 19: 65-112.
- [33] Staneva, J. V., Dietrich, D. E., Stanev, E. V., Bowman, M. J. Rim current and coastal eddy mechanisms in an eddy resolving Black Sea general circulation model, J. Mar. Syst., 2001, 31: 137-157.

#### DOI: 10.1016/S0924-7963(01)00050-1

- [34] Oguz, T., Malanotte Rizzoli, P., Aubrey, D. Wind and thermohaline circulation of the Black Sea driven by yearly mean climatological forcing, J. Geophys. Res., 1995, 100: 6846-6865.
- [35] Stanev, E.V., Staneva, J., Bullister, J. L., Murray, J. W. Ventilation of the Black Sea pycnocline. Param-

eterization of convection, numerical simulations and validations against observed chlorofluorocarbon data, Deep-Sea Res., Part I, 2004, 51: 2137-2169.

#### DOI: 10.1016/j.dsr.2004.07.018

[36] Knysh, V. V., Korotaev, G. K., Moiseenko, V. A., Kubryakov, A. I., Belokopytov, V. N., Inyushina, N. V. Seasonal and interannual variability of the Black Sea hydrophysical fields reconstructed from 1971-1993 reanalysis data, Izv. Atmos. Oceanic Phys., 2011, 47(3): 399-411.

#### DOI: 10.1134/S000143381103008X

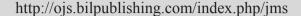
[37] Besiktepe, S. T., Lozano, C. J., Robinson, A. R. On the summer mesoscale variability of the Black Sea, J. Mar. Res., 2001, 59: 475-515.

#### DOI: 10.1357/002224001762842163

- [38] https://news.agu.org/press-release/warmer-winters-are-changing-the-makeup-of-water-in-black-sea/(accessed on 23.10.2020).
- [39] https://marine.copernicus.eu/rim-current-variations-in-the-black-sea/ (accessed on 27.10.2020).



#### **Journal of Marine Science**





#### ARTICLE

#### Research on Marine Pollution Problems and Solutions in China from the Perspective of Marine Tourism

#### Yuxiang Zheng Dandan Liu\*

School of Economics and Management, Shanghai Maritime University, Shanghai 201306, China

#### ARTICLE INFO

Article history

Received: 12 November 2020 Accepted: 30 November 2020 Published Online: 31 January 2021

Keywords:
Marine tourism
Marine pollution
White pollution
Restrictive bottleneck

#### ABSTRACT

Based on the perspective of marine tourism, this paper integrates various types of marine pollution, and puts forward high-quality development solutions and future extension direction of marine tourism. Through the research, it is found that the main culprits of marine pollution mainly include the following seven points: human activities produce garbage; white pollution; ship pollution; exploration of marine oil and gas resources and mineral pollution; land reclamation; pollution in mariculture industry and new estrogen pollution. The causes of marine pollution and countermeasures are discussed.

#### 1.Introduction

#### 1.1 Development Status of Marine Tourism

Marine Tourism refers to a series of activities such as marine travel, entertainment, and vacation based on the ocean and meeting people's spiritual and material needs under certain social and economic conditions <sup>[1]</sup>. According to the distance of the road area as the classification standard, it can be divided into coastal tourism, offshore maritime tourism and ocean tourism <sup>[2]</sup>. At present, coastal tourism is the dominant tourism mode in China.

At present, the marine tourism industry occupies a pivotal position in the world tourism industry. Coastal

countries and regions account for 23 of the top 25 tourism revenues in the world. It can be seen that coastal countries and regions play a significant role in the development of marine tourism. In Spain, Australia and other countries, marine tourism has become an important pillar industry of the national economy. Tropical and subtropical regions have formed many world-class marine tourism destinations, occupying a dominant position in the world marine tourism industry. With the continuous update of tourism products and the gradual maturity of the tourism market, the world's marine tourism industry will show a development trend of diversification, ecology, leisure and innovation.

Dandan Liu,

School of Economics and Management, Shanghai Maritime University, Shanghai 201306, China;

E-mail: 115937560765@163.com

Funding

National Social Science Fund project (19BJY208) Research on the Innovation Model of High Quality Development of China's Marine Tourism Industry under the Background of Consumption Upgrade.

 $<sup>*</sup>Corresponding\ Author:$ 

## 1.2 Marine Tourism Shifts to High-quality Development

According to the "World Tourism Economy Trend Report (2020)", the total number of global tourism (including domestic and inbound and outbound tourists) in 2019 was 12.31 billion, and the total international tourism revenue was US\$5.8 trillion [3]. The output value of China's coastal tourism industry has been steadily increasing year by year, and by 2019, it achieved an add value of 188.6 billion yuan. Although the output value of coastal tourism will decline in 2020 due to the impact of the New Crown Pneumonia Virus, tourists will retaliate consumption with the development of the new economic normal after the epidemic. The marine tourism industry will usher in a new round of development and reform. In the future, the marine tourism industry will develop in a more casual, smarter, and more humane direction. The proportion of self-guided tours and self-driving tours will increase significantly. With the development of 5G, the promotion of smart tourism applications such as VR tourism and cloud tourism will also accelerate significantly.

## 1.3 Marine Pollution-The Bottleneck Restricting the Development of Marine Tourism

Marine pollution refers to pollution caused by humans changing the original state of the ocean, destroying the marine ecosystem and causing harmful substances to enter the marine environment. The lack of supervision of land-based sewage outlets, and the large amount of waste generated by human life flowing into the ocean; the development of traditional marine industries such as coastal tourism has caused very serious white pollution to the ocean; the inefficient use of fishery resources, worn

fishing ropes, fishing nets and worn-out fishing gear being thrown into the ocean, causing seawater pollution, lack of supervision of marine fishery fishing operations, excessive pollution in the marine aquaculture industry, serious seawater eutrophication; substandard oil and sewage discharge from ships, frequent oil leakage problems; oil and gas resource exploration and exploitation technology immature, limited exploration scale, low efficiency and serious pollution; land reclamation has caused serious damage to the ecosystem, the hydrodynamic environment has been changed, and the ecological carrying capacity has declined; the discharge standards for estrogen substances have not yet been perfected, all of which are harmful to the marine tourism industry development has serious impacts, and the potential threats to the marine ecological environment and humans are immeasurable.

According to data from the State Oceanic Administration, in 2019, the sea areas under Chinese jurisdiction (the Bohai Sea, the Yellow Sea, the East China Sea, and the South China Sea) have a total area of 89,670 square kilometers <sup>[4]</sup>. At present, the water quality in the coastal waters of Shanghai and Zhejiang is relatively good. As a national key tourist city and the largest cruise home port in Asia, it is necessary to fully implement the maritime application management system, focus on solving the coastal water management problem, and effectively protect the marine ecological environment.

#### 1.4 Review of research status at home and abroad

This article focuses on the high-quality development of marine tourism and its constraints, mainly studying marine pollution and its impact. After clearly defining the concept and category of the research object, this article determines the keyword list as shown in Table 1.

keywords Marine pollution Marine travel Ocean travel Beach recreation Micro-plastic marine litter Coastal pollution Or Coastal Tourism Or plastic plastic debris Maritime shipping Coastal resources; Fibres Ocean pollution Marine plastic debris Storm-water pollution

Table 1. Keyword search plan list

The second step is research positioning. This article first chooses to search online from the SSCI and SCI core databases in Web of Science. Based on the table keyword search plan, search by subject. The collection time is up to March 2020, and the papers are selected article. After deleting conference documents, books and other informal documents, and excluding duplicate documents, a total of 68 English documents were collected in this process. The third step is to evaluate and select. First, read the title and abstract of the literature, and select the literature based on the following principles: (1) Eliminate relevant papers that study chemicals or microorganisms in the ocean; (2) Pay attention to marine pollution or the relationship between marine pollution and economic development; (3) Non-academic documents such as book reviews, editorials, and journal solicitation. In accordance with the above principles, 54 relevant documents are published and 14 are remaining. Secondly, manually search the mainstream high-quality journals in the field of "marine environmental protection" from Wanfang database, such as Journal of Oceanography, Ocean Science, Journal of Ocean University of China, Marine Environmental Science, etc., to consult and supplement the literature 2 articles related to marine pollution in these journals. Through the above process, this paper finally obtained 16 documents.

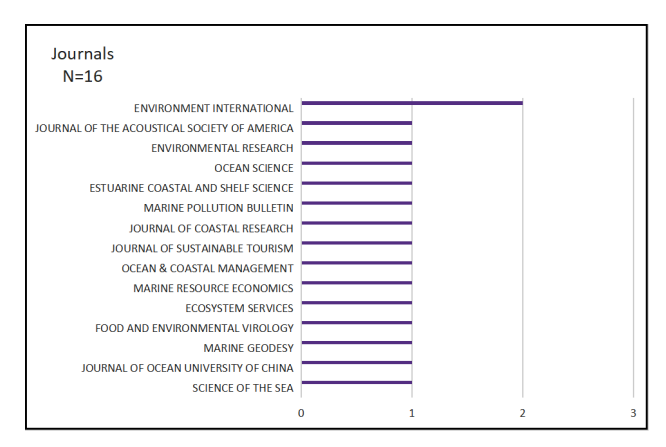


Figure 1. Main sources of literature journals

There are many factors in the causes of marine pollution, but most domestic and foreign scholars mainly discuss from one aspect of marine pollution, and the research mainly focuses on marine plastic pollution and the impact of environmental pollution on the economy. At present, the problem of marine pollution is mainly focused on microplastics pollution and the impact on marine life. Typical research results mainly include 7 articles. It can be seen that most scholars are focusing on the impact of microplastics on marine life, and the research focuses on marine pollution. There are five articles related to economic development, one article researching noise pollu-

tion, and one review article. The journal sources of 16 articles are shown in Figure 1. Two of the articles reviewed in this article are from Environment International, and the remaining articles are from Marine Science, Journal of Ocean University of China, Marine Geodesy, Food and Environmental Virology, Journal of the Acoustical Society of America, Ecosystem Services, Marine Resource Economics, Ocean&Coastal Management, Journal of Sustainable Tourism, Journal of Coastal Research, Environment Research, Marine Pollution Bulletin, Estuarine Coastal and Shelf Science, Ocean Science, four articles published in 2017 Articles, there are only two articles in 2020. It can be seen that there have been few studies on marine pollution in recent years.

Marine pollution not only affects the balance of the marine ecosystem, but also severely limits the sustainable development of China marine tourism industry. Therefore, we should pay more attention to the problem of marine pollution, make rational use of resources, and promote the high-quality development of marine tourism. Through research, this article found that the types of marine pollution mainly include the following: Human activities produce garbage; White pollution; Ship pollution; Exploration of marine oil and gas resources and mineral resources; Land reclamation; Pollution in mariculture industry; New estrogen pollution. The sources and methods of each type of pollution are different, as shown in Table 2.

#### 2. Types of Marine Pollution

#### 2.1 Human Activities Produce Garbage

The sources of waste generated by human activities mainly include industrial waste, domestic waste and medical waste. The marine pollution caused is mainly discharged through coastal sewage outlets, dumped into the ocean, merged into the ocean through rivers, and deposited in the atmosphere. According to data released by the Ministry of Ecology and Environment in 2019, large and medium-sized cities generated 1.55 billion tons of general industrial solid waste, 21.473 million tons of domestic waste, 817,000 tons of medical waste, and monitored 453 pollution source discharge outlets. The comprehensive sewage outlet has the largest discharge volume, the industrial pollution source is the second, and the domestic pollution source is the smallest [5]. The discharge points of waste into the sea are mainly land-based sewage outlets. Generally, shore discharge and offshore deep-sea discharge are selected [6]. It can be seen that the supervision of pollution source discharge outlets should be strengthened, and waste discharge standards should be strictly controlled. In addition, nutrients, heavy metal

Table 2. Causes of marine pollution

Types of marine pollution		Source of pollution	Pollution patterns			
		Industrial waste	Land source sewage outfall	Shore discharge Offshore deep sea emissions		
Human activities produce garbage		Household garbage	Dump directly			
		Medical waste	Rivers car	ry pollutants		
		Medical waste	Atmospher	ric deposition		
		Land source input	Wind action, rain w	ashing, surface runoff		
		Coastal tourism	Tourists	discarded		
White pollution		Ship transportation	Ship transpo	ort and discard		
		Fishing and breeding	Damaged and abandoned plastic fishing gear			
	Α	atmospheric deposition	Fiber sedimentation			
Ship pollution	Cruise ship  Solid Waste  Oily sewage and toxic gas  Tanker		Operational contamination			
				Shipwreck(oil spill)		
			Mude	dy sand		
Exploration of marine oil and gas resources and mineral resources	Development and mining of solid mineral resources		Improper handling of chemical substances, releasing radioactive substances			
			Sand disaster			
Land reclamation		Land reclamation	Change coastal structure and tidal movement characte			
Land rectamation		Land rectamation	Changes in the hydrodynamic environment			
		Nutrients				
Pollution in mariculture industry		Sulfide	The discharge of Nitrogen (N), Phosphorus (P), Chemical Oxygen Demand (COD), etc. leads to hypoxia			
		drug				
N		Industrial production	River and lak	e transportation		
New estrogen pollution		human activity	Atmospheric deposition			

elements, and acid rain can be imported into the ocean through atmospheric deposition and have a greater impact on the ocean

The industry directly affected by garbage discharge to the ocean is marine tourism. Cultivating environmental awareness, rationally discharging garbage, creating a green marine tourism atmosphere, and promoting the high-quality and sustainable development of marine tourism require the joint efforts of all members of society.

#### 2.2 White Pollution

White Pollution is an image term for the phenomenon of waste plastics polluting the environment. It refers to the pollution caused to the ecological environment by plastic products that are randomly thrown away after use and are difficult to degrade. Its pollution sources to the ocean mainly include: land-based input, coastal tourism, ship transportation, fishing and breeding, atmospheric deposition. According to the Bulletin of the State of China's Marine Ecological Environment in 2019, tourism and leisure areas, agriculture and fishery areas, port and shipping areas and adjacent sea areas are the areas with the most marine debris distribution. Among them, floating garbage on the sea, beach garbage and seabed garbage, plastic garbage accounted for 84.1%, 81.7% and 92.6% respectively [4]. The beach and the sea are areas with a high concentration of tourists, and are the "front" of marine tourism. Therefore, the degree of environmental protection of beaches and sea areas directly affects the development of marine tourism. It can be seen that white pollution is an important factor hindering the development of marine tourism. Strengthening sea surface supervision, improving environmental protection measures, and improving the quality of tourists are to reduce white pollution.

Land-based input is the main pollution source transported from rivers to the ocean. It is washed by wind, sewage and rain, and enters the river and marine environment through surface runoff, which causing pollution. Due to the current monitoring data in China, it is impossible to estimate the flux of marine plastic waste input and the sources of plastic waste in different marine activities [7]. So we searched for ocean plastic pollution in foreign countries. According to the 2020 report of the International Union for Conservation of Nature (IUCN), 12 million tons of plastic are leaked into the ocean every year [8]. According to a survey conducted by Schmidt and his team in 2018, rivers dump 0.47 to 2.75 million metric tons of plastic into the ocean every year, and more than a quarter of plastic waste flows into the ocean from 10 rivers, 8 of which are in Asia [9].

At seaside tourist attractions such as densely popu-

lated beaches, tourists discarded plastic packaging bags, mineral water bottles and other plastic garbage, forming microplastics into the marine environment, and causing marine pollution <sup>[10]</sup>. The discarding of plastic garbage into the ocean by passing ships at sea is also an important source of white pollution. According to UNEP estimates, the amount of plastic garbage imported into the ocean during global ship transportation in 2005 reached 5 million tons <sup>[11]</sup>. The specific classification and pollution methods of ship pollution will be discussed in detail in the next section.

In fishing activities, worn fishing ropes, fishing nets and worn-out fishing gear will be thrown into the ocean, thereby increasing the content of microplastics in the waters. The 2019 "Marine" Ghost Fishing Gear "Pollution Research Report" shows that there are about 800,000 tons of fishing gear debris discarded in the ocean every year, accounting for 10% of the total marine plastic pollution [12]. Fishing gear fragments are extremely harmful to marine biodiversity. Marine life may be entangled in fishing gear and unable to get out and eventually lead to death, causing damage to the marine ecological balance and hindering the development of submarine tourism.

Another important source of marine plastic pollution is atmospheric deposition. Dris et al. analyzed the composition of atmospheric sediments and found that 50% are natural fiber sediments, 21% are artificially processed natural fibers, 17% are man-made plastic fibers, and 12% are man-made mixed fibers [13]. This proves that fiber sediment can also cause marine pollution.

#### 2.3 Ship Pollution

Ship pollution refers to the entry of various harmful substances into the ocean due to ship manipulation, maritime accidents, and dumping at sea via ships, thereby disrupting the balance of the marine ecosystem. Marine ship pollution mainly includes cruise ship pollution and tanker pollution. There are two main ways of pollution:operational pollution and sudden pollution. Operational pollution is mainly the pollution produced by the ship in the process of traveling, and the sudden pollution is the pollution caused by the sudden maritime accident of the ship during the traveling.

#### 2.3.1 Cruise Ship Pollution

The main sources of pollution from cruise ships are domestic garbage, sewage, and solid waste. According to its source, it can be divided into four types: black water, gray water, oily bilge water and ballast water [14]. Black water, that is untreated ship sewage, generally consists of

medical waste and human waste [14]; gray water generally comes from showers, sinks, and dishwashers; marine fuel oil and mechanical waste such as engines and steam engines form oily bilge water; cruise ship ballast water is the water loaded to ensure the balance of the cruise ship. Solid waste mainly includes many domestic wastes such as plastic waste and food waste.

According to foreign data, a cruise ship will produce approximately 50 tons of garbage, 1 million US gallons of gray water, 210,000 US gallons of sewage and 25,000 US gallons of oily water during a one-week journey [15] (according to Chinese national standards GB3102.1-1993, 1 gallon (US) = 3.785412 liters). Different from landbased pollution, the waste discharge supervision of marine cruise ships is insufficient, and the detection technology is immature. Due to the uncontrollability of cruise ships, it passes through multiple countries and regions each time, and the laws and regulations of each country and region have different sewage discharge standards that cannot be unified. The development of cruise tourism has been booming in recent years. On October 19, 2019, China's first large-scale domestic cruise ship officially started construction and is scheduled to be delivered and operated in 2023. Once cruise tourism develops in China, cruise pollution is an inevitable topic. Therefore, we should realize that the solution to the problem of marine pollution is imminent.

#### 2.3.2 Tanker Pollution

The main sources of oil tanker pollution are oily sewage, toxic liquids, and marine accidents (oil spills). The oily sewage, ballast water, and tank washing water of oil tankers contain a large amount of oil. Emergency discharge of cargo and oil spills from tanker cargo warehouses will cause toxic liquid leakage. Excessive oily sewage discharge will cause marine pollution. At present, each country has its own oily sewage discharge standards, but in view of the wide range of coverage and poor operability, it is difficult to implement. Oil spill-the super killer of the marine environment, its pollution is mainly sudden pollution. After the toxic compounds contained in oil leak into the ocean, they quickly enter the food chain, and no creatures from lower to higher are immune. It will have a serious impact on the marine tourism industry, especially the cruise tourism industry.

According to statistics, the amount of oil and petroleum products released into the ocean through various channels amounts to 2 million to 10 million tons each year. The petroleum pollutants discharged into the ocean by shipping amount to 1.6 million to 2 million tons, and the most prominent pollution is caused by the death of a tanker <sup>[16]</sup>. There are about 500 marine oil spill accidents in China every year. Oil will form a large area of oil film on the sea, causing serious marine pollution, destroying the marine ecological environment, and causing serious impact on marine tourism. At present, the main methods of dealing with the leakage of offshore crude oil include oil containment method, combustion method, dispersant method, adsorption method, and microbial ingestion method <sup>[17]</sup>. But no matter which method has its own advantages and disadvantages, the degree of recovery of the marine environment is also different. Once an oil spill occurs, the pollution to the ocean is still serious and difficult to predict. Therefore, rather than remedial measures, it is more important to prevent problems before they occur.

## 2.4 Exploration of Marine Oil and Gas Resources and Mineral Resources

The ocean has very rich resources-oil and gas resources and mineral resources. According to the assessment of the United States Geological Survey (USGS), the world (excluding the United States) has 54.8 billion tons of undiscovered petroleum resources (including condensate) and undiscovered natural gas resources. 78.5 trillion cubic meters [18], there are 7 sedimentary basins with petroleum prospects in China, with a total area of about 700,000 kilometers. Therefore, China's marine oil and gas resources and mineral resources have huge development potential, and prospects for exploration are good.

The comprehensive indicator of China's marine development is 3.4%, mainly based on mineral resources [19]. China is still immature in terms of mineral resource mining technology and laws and regulations. Uncontrolled mining and irregular systems have led to serious environmental pollution problems, muddy seabed sediments, improper handling of chemical substances in mineral resources exploration, and release of radioactive substances, these will threaten the survival of marine life. For example, in the mining of seaside placers, due to the imperfect system and immature technology, uncontrolled mining leads to waste and serious environmental pollution [20]. Therefore, it is necessary to formulate corresponding laws, regulations and policies, increase government intervention, cultivate talents related to marine resource exploration, improve mining technology, and carry out sustainable mining.

#### 2.5 Land Reclamation

Land reclamation refers to the act of transforming the original sea area, lake area or river bank into land through artificial technology. From the 1950s and 1960s, China began to reclaim land from the sea. By the end of the last

century, the area of land reclamation from the sea reached 12,000 square kilometers. Land resources continue to be in short supply, and the new impetus to promote economic growth in coastal areas has become a demand for land from the sea. However, uncontrolled and unscientific continuous reclamation of the sea will change the coastal structure and hydrodynamic environment, and marine resources will be drastically reduced. Large-scale reclamation activities not only affect important ecosystems such as coastal wetlands, mangroves, and bays, but also destroy the habitats of marine life, resulting in a significant reduction in biodiversity. The destruction of oceans and marine resources by reclamation activities and becoming more and more scarce, how to talk about the development of marine tourism.

#### 2.6 Pollution in mariculture industry

In recent years, China has moved from rapid development to an era of high-quality development. People's income levels have continued to increase, and the types of seafood have become more and more abundant. The production of crustaceans and shellfish has increased year by year, accounting for 79.47% of the total, as shown in Figure 2, the composition and proportion of national fishing in 2016 to 2018. Although the proportion of marine fishing has been declining year by year, it can still be clearly seen that marine fishing accounts for as much as 70% of the national fishing. The increasing amount of seafood farming has caused serious pollution in offshore waters. The seawater has become eutrophic, and the spawning grounds and habitats of fishery organisms have been destroyed, which has seriously affected the water environment of the offshore waters and the sustainable development of coastal tourism.

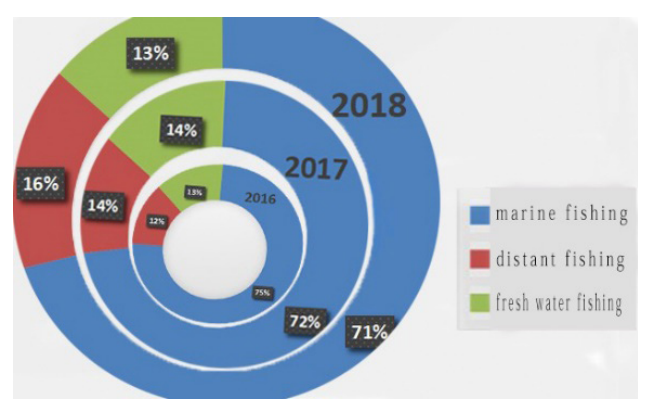


Figure 2 Fishing composition and proportion in 2016-2018

Data source: China Fishery Statistical Yearbook 2019

Mariculture can cause serious chemical pollution [21].

Nutrient salts and other components will be deposited on the bottom of the water, resulting in hypoxia, which is not conducive to the growth of marine life and causes serious marine pollution. The marine environment is closely related to the survival of organisms, and it is also related to the long-term development of marine tourism. Therefore, it is very important to do a good job in the prevention and control of pollution in the marine aquaculture industry, establish a reasonable marine aquaculture plan, unify marine aquaculture specifications, and cut off the source of pollution. Only in this way can we better protect the marine environment and promote the ecological and healthy development of marine tourism [22].

#### 2.7 New Estrogen Pollution

The last type of marine pollution-New Estrogen pollution. Environmental Estrogens refers to the presence of chemicals in the environment that have estrogen-like effects in the body or block the effects of androgen [23]. After it enters the body, it can interfere with the synthesis, release, transportation, binding, and metabolism of normal endocrine substances in the body, thereby destroying the compounds that maintain the stability and regulation of the body, and produce various toxic effects on the organism. It belongs to environmental endocrine disruptors [24].

Estrogen substances enter the environment, enter the marine environment through the transportation of rivers, lakes, and atmospheric deposition. After being absorbed by marine organisms, they will in turn endanger humans. At present, most new estrogens lack a regulatory mechanism and have not formed a corresponding environmental standards [25]. In recent years, research on new estrogen in foreign countries has gradually increased, but domestic research is relatively insufficient. Therefore, the improvement of new estrogen-related emission standards, the study of the migration law of new estrogen in the ocean and the impact on humans, are important for protecting ocean water. The development of resources, environment, marine tourism, and human physical and mental health have very important practical significance.

#### 3. Causes of Marine Pollution

China's current laws and regulations on the discharge of marine garbage are not perfect, the relevant departments have insufficient supervision, the incomplete establishment of supervisory institutions, the lack of personnel and the inability to fundamentally implement the responsibility of ecological environmental protection; the prevention and control of land-based pollution is relatively difficult, and it is difficult for the sewage outlets to enter the sea. Inadequate supervision of rivers requires

coordinated treatment of industrial pollution, agricultural pollution and many other sources of pollution, which has increased the difficulty of treatment. The sources, types and quantities of marine garbage are not monitored in place. The waste recycling industry chain has not yet been formed, and garbage treatment technology needs to be improved; in some coastal areas, the illegal discharge of black water and garbage enclosing the sea are prominent and have not been effectively resolved, which seriously affects the publics quality of life and tourist pro-sea demand; some companies fail to assume the responsibility for ecological and environmental protection. Production and neglect of environmental protection. In order to reduce costs, equipment processing waste materials are not up to standard, stolen to the sea and leaked to the sea, illegally exploited in marine protected areas, sea sand areas, etc.; beach garbage classification measures are not yet complete, cruise waste disposal supervision is insufficient, tourists are in the ocean ecological and environmental protection awareness is still insufficient, self-discipline needs to be improved, and green and sustainable lifestyles and consumption patterns need to be formed. These series of factors have caused pollution problems in the ocean.

#### 4. Solutions

## 4.1 Improve Laws and Regulations and Strengthen Supervision

As the main body, the government should promulgate corresponding laws and regulations to control the total discharge of marine pollutants, and place marine environmental protection work in key and prominent positions [26]. Establish relevant regulatory departments, improve marine garbage discharge standards, and formulate mandatory measures and punishment mechanisms to restrict people's dumping of marine garbage, minimize the impact of man-made marine pollution, and effectively protect the marine environment [27]; relevant enterprises perform their own obligations to achieve transparency in their waste discharge; increase maritime law enforcement agencies to supervise various marine activities and rationally use marine resources; make corresponding regulations on the scope of fishery and aquaculture seawater, and establish aquaculture standards, and regulate plastic fishing gear carry out unified recycling and reuse, and fully implement the responsibility of protecting the ecological environment of the sea.

### 4.2 Strengthen Publicity and Raise Public Environmental Awareness

Raise the public's awareness of marine ecological and

environmental protection, conduct marine environmental protection publicity and corresponding training, make the public aware of the harm caused by marine pollution, and actively participate in marine environmental protection activities. Learn from Japanese garbage classification and recycling measures, encourage the public to consciously carry out garbage classification and recycling, and organize the cleanup of garbage on the beach. Conduct marine environmental protection education for young people to form a green lifestyle and consumption model. Citizen travel should be a behavior that relieves their own pressure and is conducive to economic growth. They should respect the construction of the local ecological environment, minimize damage to the environment, and carry out sustainable and responsible tourism.

## **4.3** Use New Technologies to Promote the High-quality Development of Marine Tourism

Based on the scientific development background, the use of marine environmental pollution information intelligent image detection technology to monitor the source, type, quantity and destination of marine garbage [28]; innovative development models such as "Marine Tourism + Internet", "Marine Tourism + Big Data", promote sustainable tourism, eco-tourism and other tourism concepts, improve tourism quality, and promote the construction of smart marine tourism; improve the marine intelligent monitoring platform, use big data technology, VR technology, etc. So as to realize the sharing and coordination of marine resources. In the future, the marine tourism industry will pay more attention to the personal experience of tourists and meet the needs of tourists' participation. Innovative tourism experiences such as underwater adventures and robot guides will be satisfied. Live tourism, tourism product delivery, full-time tourism, educational tourism, etc. This traveling methods will appear. With the development of 5G, the advancement of smart travel applications such as VR travel and cloud travel will also be greatly accelerated.

#### 5. Conclusion

In the past ten years, as the country's economic strength has continued to increase, China has moved from rapid development to an era of high-quality development. The economic structure is undergoing tremendous changes, and tourism has become a normal and rigid demand for the people. However, for a long time, marine pollution caused by wanton destruction of the marine environment has seriously hindered the development of marine tourism. The innovation of this article is to explore the seven

sources of marine pollution and pollution methods from the perspective of the bottleneck of marine tourism development. Activities generated garbage; white pollution; marine ship pollution; marine oil and gas resources and mineral resources exploration pollution; land reclamation; marine aquaculture industry pollution; new estrogen pollution, and studied the causes of marine pollution and solutions. In addition, we proposed the future direction and goals of high-quality development provide important support for the realization of a maritime economic power and the development of sustainable marine tourism.

#### References

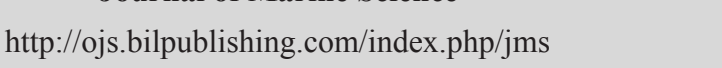
- [1] Jian Gao. Discussion on the development model of island tourism[D]. Master's degree thesis of Zhejiang University, 2007.
- [2] Xin Li, Yunpeng Sun. Analysis of the development status of my country's marine tourism industry[J]. Journal of Tangshan Normal University, 2009, 31(01): 105-107.
- [3] WTCF. World Tourism Economic Trend Report[EB/OL].[2020-03-06]; Available from:
  https://mp.weixin.qq.com/s?src=11&time-stamp=1589441697&ver=2337&signa-ture=Qu0-BPZGzfTNDMn4-2wlWAP9Ycrv\*5HC-jle8fVsDoMz5P5A8O-vjw8hVidVFBbbF6f1gwpX-8b7RcI4QS3QRNxqmugB0YCDymnUnNyyTmZ-cAFgXGnewbj=1LsZOQ44
- [4] State Oceanic Administration. Bulletin of China's Marine Ecological Environment [EB/OL]. [2020-06-13]; Available from: http://www.mee.gov.cn/hjzl/sthjzk/jagb/
- [5] Ministry of Ecology and Environment. National Annual Report on the Prevention and Control of Solid Waste Pollution in Large and Medium-sized Cities [EB/OL]. [2019-12-31]; Available from: http://www.mee.gov.cn/hjzl/sthjzk/gtfwwrfz/
- [6] Limin Yu, Zhifeng Zhang, Zhongsheng Lin, et al. Research on the multi-level classification system of land-source sewage outfalls[J]. Ocean Development and Management, 2013, 30(06): 73-76.
- [7] Juying Wang, Xinzhen Lin. Analysis of ocean governance system to deal with plastic and microplastic pollution[J]. Pacific Journal, 2018, 26(04): 79-87.
- [8] Sousa, J. The Marine Plastic Footprint report: calculating the millions of tonnes that end up in the oceans[EB/OL]. [2020-02-04]; Available from: https://www.iucn.org/news/marine-and-polar/202002/marine-plastic-footprint-report-calculating-millions-tonnes-end-oceans
- [9] Schmidt. Plastic from source to sea rivers: conveyors

- belts of plastic pollution[EB/OL]. [2018]; Available from: https://www.iucn.org/
- [10] Bin Xia, Yushan Du, Xinguo Zhao, et al. Pollution status and biological effects of microplastics in marine fishery waters[J]. Advances in Fisheries Science, 2019, 40(03): 178-190.
- [11] UNEP. Marine litter: An analytical review[EB/OL]. [2005]; Available from: https://www.iucn.org/
- [12] Non-governmental organization World Animal Protection Association. Abandoned fishing gear harms the ocean: Every day in Brazil can produce 580 kg [EB/OL]. [2019]; Available from: http://news.chinaxiaokang.com/guoji/ 2019/0403/657832.html
- [13] Rachid D, Johnny G, Mohamed S, Cécile M, Bruno T. Synthetic fibers in atmospheric fallout: A source of microplastics in the environment?[J]. Marine Pollution Bulletin, 2016, 104(1-2).
- [14] Fangyuan Lu. Research on the legal issues of cruise ships from the perspective of transportation[D]. Doctoral Dissertation of Dalian Maritime University, 2015.
- [15] Kira Schmidt. Criminal Cruise Ships: Soiling the Seven Seas[J]. EARTH ISLAND, 2000.
- [16] China Environment News. What are the hazards of marine oil pollution? [EB/OL].[2015]; Available from: http://www.hycfw.com/Article/65920.
- [17] Liting Nong. Talking about the treatment method of
- marine crude oil leakage[J]. Chemical Management, 2016(20): 281.
  [18] China Petroleum and Chemical Network. Invento-
- [18] China Petroleum and Chemical Network. Inventory of the four emerging areas of global deepwater oil and gas exploration [EB/OL]. [2016]; Available from:
  - http://www.chemall.com.cn/chemall/infocenter/newsfile/2016-7-11/2016711112238.html
- [19] Chunmei Cheng. Discussion on the status quo of marine resource development and pollution analysis[J]. Resource Conservation and Environmental Protection, 2015(07): 144.
- [20] Kejing Li. Development status and sustainable development strategies of marine mineral resources[J]. Great Science and Technology, 2016(27): 332-332.
- [21] Dongtao Deng, Jiasen Zhu, Yehua Liu. Environmental pollution of marine aquaculture and improvement measures[J]. Regional Governance, 2018(6): 65.
- [22] Xijia Xu, Huajun Bao. Environmental pollution of marine aquaculture and its control countermeasures[J]. Agricultural Technology Service, 2017. 34(22):161.

- [23] Xin Lei, Zhenmin Lian, Li Cao, et al. The mechanism of action and toxicity detection of environmental estrogens[J]. Journal of Yan'an University (Natural Science Edition), 2005. 24(3): 68-70.
- [24] Hongyan Du. Environmental risk assessment of two new types of estrogen pollutants[D]. Nankai University, 2008.
- [25] Yuwei Shi, Ling Cai, Chenyuan Pan, et al. Research progress on pollution characteristics of new estrogen in marine environment[J]. Journal of Chemical Engineering of Chinese Universities, 2019, 33(06): 1285-1302.
- [26] Yingli Wang, Xiaoran Wang, Junjie Ge. my country's marine pollution hazards and prevention measures[J]. Resource Conservation and Environmental Protection, 2019(9): 24.
- [27] Chunxiao Wang, Longfei Zhang, Yuanyuan Xu. Analysis of pollution and treatment of marine debris[J]. Global Human Geography, 2016(6):247.
- [28] Jishun Ma, Bin Zhao, Qianwen Zheng. Analysis of Intelligent Image Monitoring Technology for Marine Environmental Pollution Information[J]. Ship Materials and Market, 2019(8): 26-27.



#### **Journal of Marine Science**





#### ARTICLE

# Microbial Communities in Water during Red Tides along the Coast of China-A Case Study of *Prorocentrum Donghaiense* Red Tide in the East China Sea

#### Bei Huang 1\* Na Wei 1 Yuheng Hu 2 Hongyue Mao 1

- 1. Zhejiang Provincial Zhoushan Marine Ecological Environmental Monitoring Station, Zhoushan, Zhejiang, 316021, China
- 2. Zhejiang Society for Environmental Sciences, Hangzhou, Zhejiang, 310007, China

#### ARTICLE INFO

Article history

Received: 27 November 2020 Accepted: 28 December 2020 Published Online: 31 January 2021

Keywords: East China Sea Red tide

Prorocentrum donghaiense High throughout sequencing

#### **ABSTRACT**

Red tides are a major public hazard in the global oceans. The coast of the East China Sea is the sea area where red tide disasters are the most frequent and serious in China. In order to accurately grasp the occurrence of red tides in the coastal waters of the East China Sea, and to understand the microbial communities in the waters during the occurrence of red tides in the East China Sea, a special survey of red tides in the coastal waters of Zhejiang, China was carried out in June 2018. The results showed that nutrient concentrations of N and P were generally high in this area, DIN concentrations in most areas exceeded the permitted limit of Chinese seawater quality grade I. There were significant differences in dissolved oxygen, pH, COD, chlorophyll and phytoplankton abundance of red tides. During the investigation, red tides were found in the waters near the Yushan Islands. The content of chlorophyll a was 42.12mg/m3, the cell abundance of phytoplankton was 8.16×108/L, and the abundance of Prorocentrum edulis accounted for 98.5%. The Illumina MiSeq sequencing platform was used for 16s high-throughput sequencing of water microorganisms, and a total of 16 bacteria were identified. Proteobacteria is the first dominant phylum, followed by Cyanobacteria and Bacteroides. Some differences in bacterial community compositions between HAB and the nearby seawater were observed. The predominant bacteria in the red tide occurrence area were Proteobacteria, comprising 46.1% of the relative abundance; while the predominant bacteria in the nearby sea area, comprising 42.0% of the relative abundance.

Bei Huang,

Zhejiang Provincial Zhoushan Marine Ecological Environmental Monitoring Station, Zhoushan, Zhejiang, 316021, China; E-mail: bighb@163.com.

Fund Project:

National Key Research and Development Program "High-resolution Numerical Simulation and Prediction of Ecological Environment in the Yellow and East China Seas" (Project No.: 2016YFC1401603); Scientific Research Project of Department of Ecology and Environment of Zhejiang Province (Project No.: 2016A012).

<sup>\*</sup>Corresponding Author:

#### 1. Introduction

Red tides are a major public hazard in the global oceans today. With the economic development of coastal areas, the occurrence of red tides in coastal waters has become more and more frequent, and the scope of occurrence and the degree of harm are also increasing. The ecological environmental damage caused by red tides has become more and more serious. It has become a marine ecological environment of general concern in the world today [1]. Influenced by several main rivers, such as the Yangtze River and Qiantang River in the north, the Taiwan warm current from the South and the southerly wind in summer, the dynamic environment of the coastal water in Zhejiang is complex, and the nutrients and biomass in the water are high, which is the most frequent and serious red tide disaster in China. The earliest record of red tide in China is the Noctiluca red tide which occurred along the coast of Zhejiang Province, China in 1933. According to the Zhejiang Marine Environment Bulletin (2000-2010) published by the Zhejiang Ocean and Fisheries Bureau and related documents, from 2000 to 2010, a total of 316 red tides were recorded in Zhejiang sea area, with a cumulative area of more than 91,000 km<sup>2</sup>. There were 57 toxic and harmful red tides, with a cumulative area of more than 2.2 km<sup>2</sup>. In 2011, the direct economic losses caused by red tide disaster in Zhejiang Province exceeded 243 million yuan. It is especially worth noting that the occurrence of toxic red tides in recent years has shown a rapid growth trend, which has caused long-term potential adverse effects on people's lives and health and the marine ecological environment, and at the same time has brought great threats to the sustainable development strategy of the marine economy [3-5].

The growth and proliferation of red tide algae are not only closely related to environmental factors, but also closely related to surrounding microorganisms. The growth and elimination of red tide algae is accompanied by the joint action of many microorganisms. Marine bacteria and algae are closely combined in space and time. They can synthesize different types of metabolites, and these metabolites can have beneficial or harmful effects on both sides <sup>[6]</sup>. Bacterial metabolites can specifically hinder or even stop the propagation of algae <sup>[7]</sup>, and may also promote the proliferation of algae. There may be some feedback mechanisms which play an important role in controlling the population dynamics of algae and marine bacteria.

Most microorganisms in the marine environment are in an unculturable state, which affects the in-depth study of environmental microorganisms [8]. Among the numerous

microorganisms, less than 1% of them can be separated by culture method [9]. Therefore, this traditional plate culture method can only be used as an auxiliary tool, and it needs to be combined with modern biotechnology methods to reflect the real information of microbial community structure more objectively and comprehensively. With the popularization of molecular biology technology in recent years, studying the diversity of microorganisms at the DNA level has become the most important technical means of current research, and has promoted the rapid development of microbial oceanography [10]. The paper uses the MiSeq high-throughput sequencing platform to conduct a comprehensive and in-depth investigation of the microbial diversity of sea water when red tides occur, and uses a variety of statistical software and other common community analysis tools to conduct in-depth research on the potential relationship between microbial communities and environmental factors, with a view to providing technical support for China's offshore ecological research and environmental management.

#### 2. Materials and Methods

#### 2.1 Sampling Overview

According to the perennial monitoring results of the Zhejiang Sea by the Zhoushan Marine Ecological Environment Monitoring Station in Zhejiang Province: the turn of spring and summer is the period of high incidence of red tide disasters in the Zhejiang sea area. The sea areas with high frequency of occurrence are mainly concentrated in the sea area near Shengsi Sea Area, Dongji Sea Area, Zhujiajian Sea Area, Xiangshan Harbo, Yushan Islands, Taizhou Islands and Nanji Islands.

In June 2018, the professional marine environment survey ship "Zhehai Environmental Supervision" was used to conduct a patrol survey of the marine ecological environment in the above sea areas. According to the occurrence of red tides at the scene over the years, a total of 12 stations have been set up. The specific locations of the survey stations are shown in Figure 1. During the investigation, a red tide was suspected to have occurred in the waters of the Yushan Islands. The water on site was dark brown, distributed in blocks, accompanied by a fishy smell.

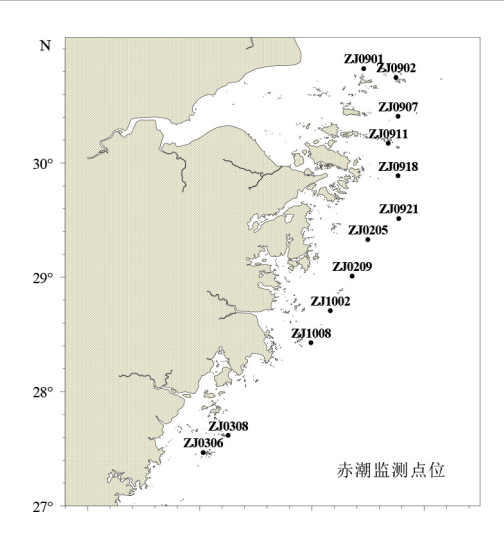


**Figure 1.** Sampling sites of high frequency area of red tide in Zhejiang sea area

#### 2.2 Sampling and Analysis Methods

Ecological environment survey: the sampling analysis and phytoplankton analysis methods of the investigated sea area ecological environment parameters are shown in Table 1.

#### 2.3 Microbial Community Analysis

Sampling water samples in areas where red tides occur and nearby sea areas to conduct microbial community analysis. The total DNA was extracted with TIANGEN TIANamp Soil DNA Kit and operated according to standard procedures. The sequencing samples were constructed by Hangzhou G-BIO Biotechnology Co., Ltd. in accordance with the 16S metagenomic sequencing standard process to construct the 16S rRNA gene V3-V4 variable

Table 1. Analyzing methods and equipment of marine ecological environmental investigations

Item	Sampling method	Analysis method	Method	Analytical Instruments	
Chlorophyll a	surface water sampling	Spectrophotometry	GB17378.7-2007(8.2)	Cary50 spectrophotometer	
Water temperature	GO-FLOW bottle	CTD Method	CTD Method GB/T12763.2-2007		
Salinity	GO-FLOW bottle	CTD Method	GB/T12763.2-2007	YSI6600 multi-parameter water quality instrument	
COD	GO-FLOW bottle	Basicity KMnO4	GB17378.4-2007(32)	VITLAB automatic titrator	
pH	GO-FLOW bottle	Glass Electrode Method	GB17378.4-2007(26)	PB-21pH meter	
Labile Phosphate	GO-FLOW bottle	Flow injection colorimetric method	EPA 365.5-1997	QuAAtro Flow Analyzer	
Nitrite Nitrogen	GO-FLOW bottle	Flow injection colorimetric method	EPA 353.4-1997	QuAAtro Flow Analyzer	
Nitrate Nitrogen	GO-FLOW bottle	Flow injection colorimetric method	EPA 353.4-1997	QuAAtro Flow Analyzer	
Ammonia nitrogen	GO-FLOW bottle	Flow injection colorimetric method	EPA 349.0-1997	QuAAtro Flow Analyzer	
Silicate	GO-FLOW bottle	Flow injection colorimetric method	EPA366.0-1997	QuAAtro Flow Analyzer	
Phytoplankton	GO-FLOW surface water extraction	Quantity: concentrated counting method	GB17378.7-2007(5)	Leica DM4000B microscope	
	Shallow water type III vertical trawl	Type: Microscope			

region (primer sequence: 341F-CCTACGGGNGGCWG-CAG; 805R-GACTACHVGGGTATCTAATCC) sequencing library of environmental microorganisms, perform corresponding quality control, and use Illumina MiSeq double-end (250 bp×2) sequencing platform to complete the sequence determination. Specific experimental procedures, quality control and sequence analysis methods can refer to Reference 11 [11].

#### 2.4 Data Processing

The analysis results of various environmental factors and phytoplankton in the seawater environment are used to draw the planar distribution map of each parameter using ODV4.0 software. Based on the 16S high-throughput sequencing results, the species composition map and Venn diagram were drawn by R language. The canonical Association (CCA) analysis was carried out with the software of Past to explore the potential relationship between phytoplankton and the environment.

#### 3. Results

#### 3.1 Sea Water Quality

A water environment survey was conducted in the surveyed sea area in June 2018. The monitoring results of the main water quality factors are shown in Table 2. The plane distribution of each factor is shown in Figure 2.

According to the national "Sea Water Quality Stan-

dard" (GB3097-1997), the measured parameters of inorganic nitrogen and active phosphate are the factors that exceed the standard of sea water quality. Among them, the concentration of inorganic nitrogen is generally higher, with an average value of 0.414 mg/L, and 91.7% of the samples exceed the first-class seawater standard. From a planar distribution, the inorganic nitrogen content in the northern waters at the mouth of Hangzhou Bay is significantly higher than other regions. The average value of active phosphate is 0.013 mg/L, and 41.7% of the samples exceed the first-class seawater standard, and the planar distribution is the same as that of inorganic nitrogen.

The single factor T test was used to investigate the results of the water quality factors to investigate the differences between the various indicators of the red tide water body and the nearby sea area. It was found that the dissolved oxygen, pH, COD, chlorophyll and phytoplankton abundance of the red tide water body were significantly different (p<0.01).

#### 3.2 Phytoplankton

A total of 56 species of phytoplankton belonging to 38 genera, 20 families and 6 phyla were identified, including 30 species of Bacillariophyta (53.6%), 21 species of dinoflagellate (37.5%), 1 specie of Chrysophyta, Euglena, Cryptophyta, Rhaphidophyta and Dinoflagellate, accounting for 1.8% respectively. The main species are Hillea sp., *Prorocentrum donghaiense, Skeletonema costatum* 

Table 2. Statistical results of major monitoring indicators

Water quality factors	Sample quantities	Range	Average value	Variance	P value (T test)
Chlorophyll a(mg/m³)	13	0.36~42.12	6.18	127.688	8.00×10-8
Number of phytoplankton species	13		75 (Total)	84.97436	0.950
Phytoplankton Abundance (×104/L)	13	0.4~816	162	5922555	5.06×10-7
Shannon index	13	0.58~3.12	1.86	0.6508231	0.182
Water temperature (°C )	13	21.2~23.7	22.3	0.925	0.467
Salinity	13	20.7~32.3	29.3	10.04333	0.507
Dissolve oxygen (mg/L)	13	6.54~15.1	8.30	5.18309	1.6×10-7
рН	13	8.03~8.60	8.20	0.0207641	5.90×10-7
Active phosphate (mg/L)	13	<0.001~0.030	0.008	9.48E-05	0.012
COD (mg/L)	13	0.36~8.29	1.31	4.603581	6.25×10-8
Dissovled inorganic nitrogen (mg/L)	13	0.051~0.998	0.414	0.09032924	0.024
Active silicate (mg/L)	13	0.311~1.26	0.648	0.09146092	0.108

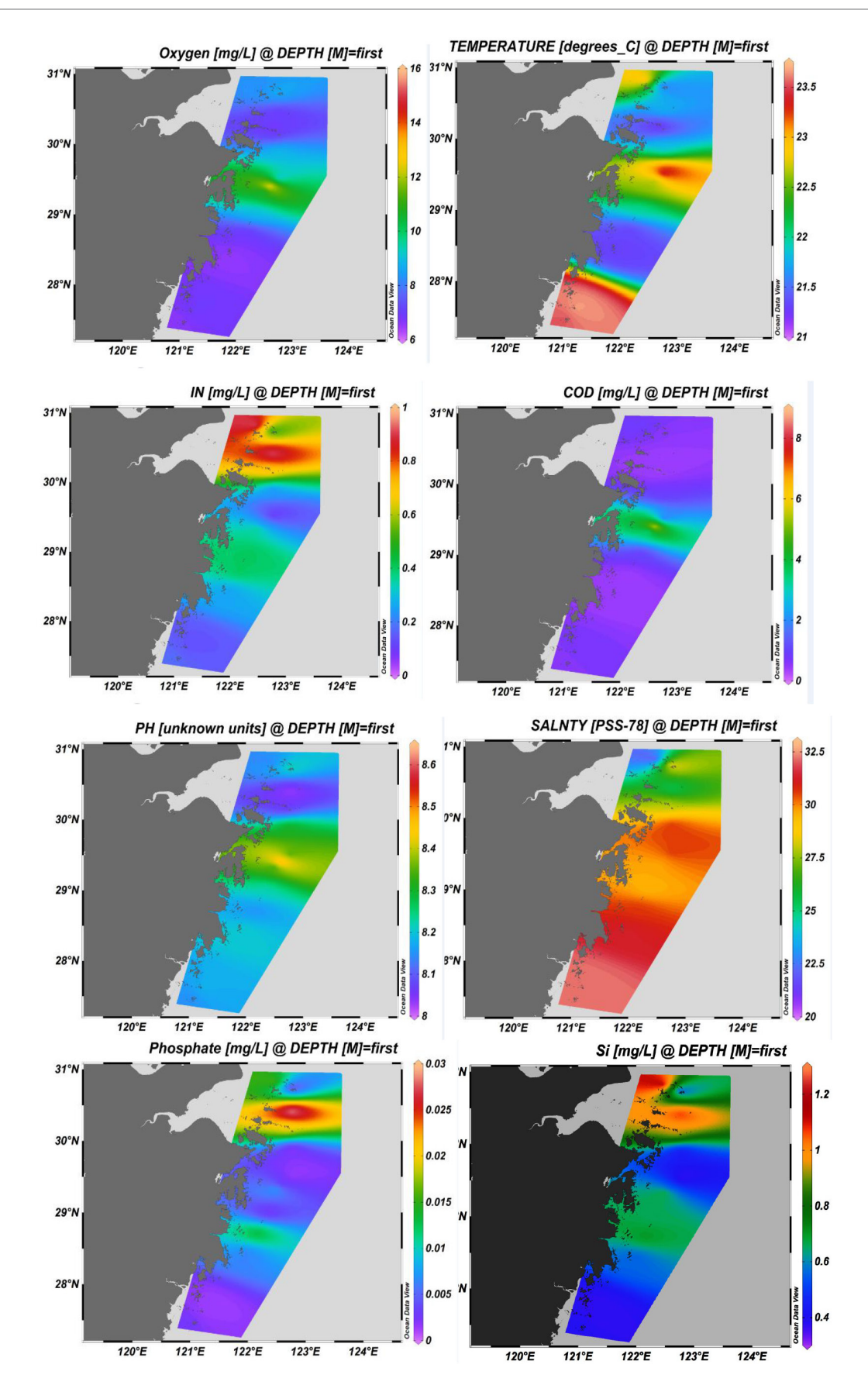


Figure 2. Distribution of main environmental factors

and so on. The average cell abundance is  $1.03\times10^5$ /L. The average content of chlorophyll a is  $3.16 \text{ mg/m}^3$ , and the middle part of the survey area is the high value sea area of chlorophyll a. The red tide was found in the sea area near Yushan Islands. In the red tide area (J2018), the content of chlorophyll a is  $42.12 \text{ mg/m}^3$ , and the cell abundance of phytoplankton is  $8.16\times10^8$ /L, of which the abundance of Prorocentrum donghaiensis accounts for 98.5%. It can be considered that this is a Prorocentrum donghaiense event.

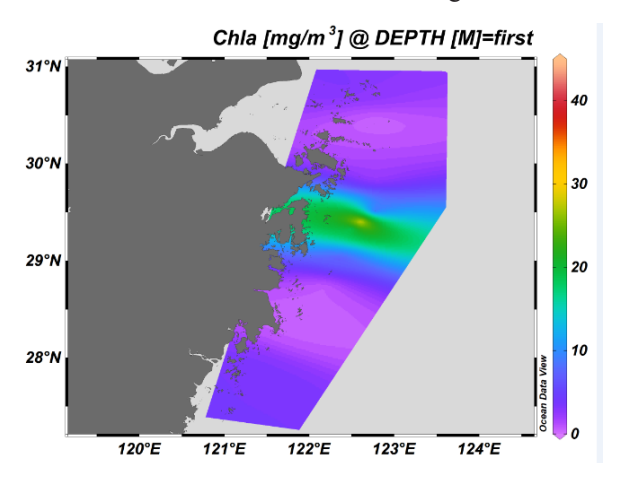


Figure 3. Distribution of chlorophyll

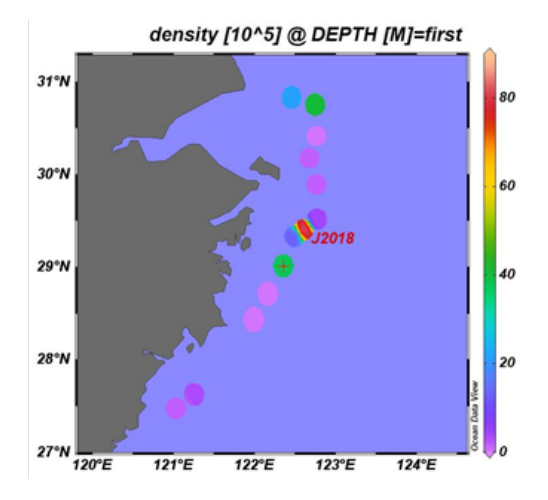


Figure 4. Phytoplankton density of monitoring sites

### 3.3 Microbial community

### 3.3.1 Sequence Statistics

High throughput sequencing based on Illumina platform was carried out to collect microorganisms in surface water of the sea area where red tide occurs (HAB01) and the sea area where no red tide occurs (ZJ0205). A total of 75451 pairs of microbial original sequences (pair-end reads) were obtained, with an average sequence length of 412 bp. After quality control and sequence optimization, 77430 high-quality sequences were selected. Considering the large differences of sequencing data at each station, further random sampling was conducted to standardize the data to balance the impact of sampling error on subsequent analysis. After preprocessing, 595 OTUs were obtained according to 97% sequence similarity. The detailed distribution of OTUs is shown in Table 3.

**Table 3.** Summary of sequence information of marine sediment microbes

Station	Original sequence	Effective sequence	Optimized sequence	Operational taxonomic units(OTUs)
HAB01	38203	37983	37540	420
ZJ0205	37248	37045	36890	505

Using mothur software to randomly sample the optimized sequences, and construct the dilution curve with the number of sequences drawn and their Chao1 index as shown in Figure 5. The results show that the curve of each station tends to be flat, indicating that the number of sequencing in this experiment is reasonable, the OTU sampling has reached or close to saturation, and the experimental results basically reflect the species diversity of the samples.

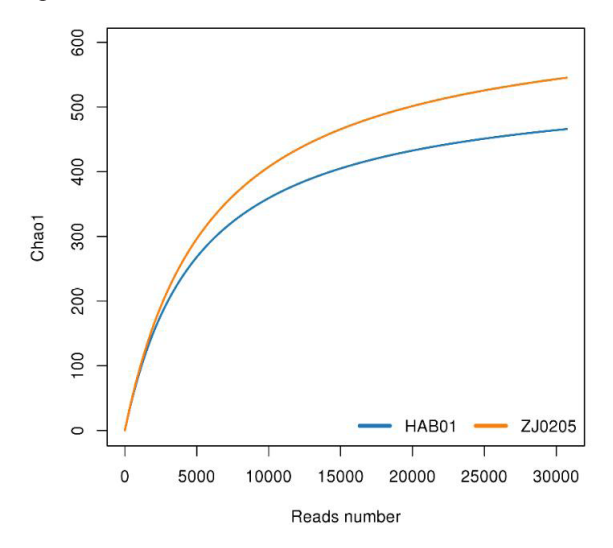


Figure 5. Rarefaction of marine sediment microbes

### 3.3.2 Microbial Species Composition

A total of 16 phyla, 82 families and 126 genera of bacteria were identified in this survey. Among them, Proteobacteria is the first dominant group, accounting for 38.4% of the total, followed by Cyanobacteria and Bacteroidetes, accounting for 29.9% and 24.3% of the total. In addition, Actinobacteria, Verrucomicrobia and Planctomycetes were also detected. The composition of microflora in the

red tide occurrence area (HAB01) and the nearby sea area (ZJ0205) is shown in Figure 6. At the level of subordination, some genera of Bacillariophyta, Candidatus Pelagibacte and Flavobacteriaceae are the main dominant genera. The composition of the main genera is shown in Figure 7.

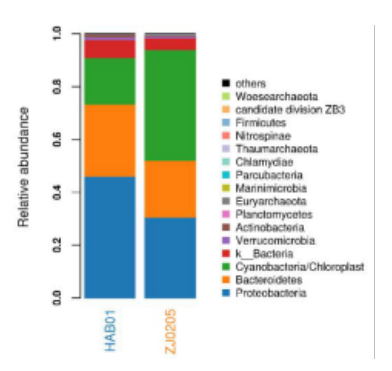


Figure 6. Species composition (phylum level)

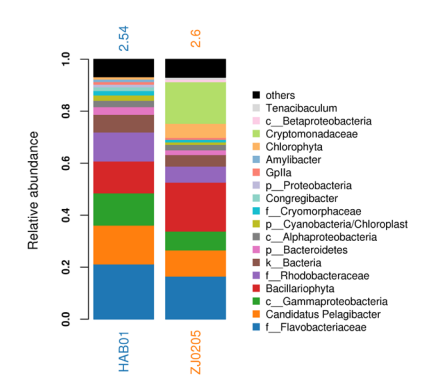
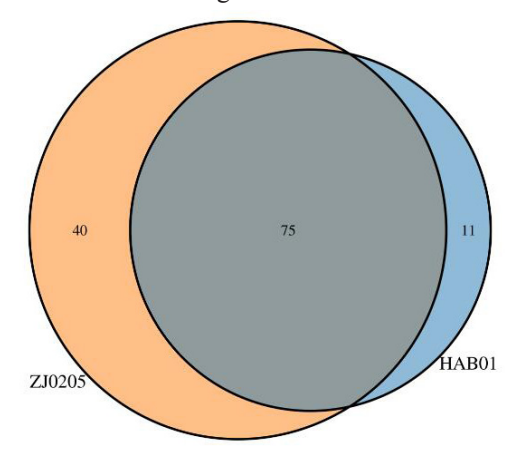


Figure 7. Species composition (genera level)

At the subordinate level, there are 75 genera of microorganisms in the two regions, accounting for 59.5%, and more than half of the total species

The Venn-Diagram diagram at the genera level was used to analyze the differences in the microbial communities between the red tide occurrence point and the nearby sea waters (Figure 8). From a genera level, there are 75 genera of microorganisms in the two regions, accounting for 59.5%, and a total of more than half of the species; 11 genera of microorganisms in the in the sea area where red tide occurs, accounting for 8.7%; and 40 genera of microorganisms in nearby waters, accounting for 31.7%. In

terms of species composition, there are nearly half of the two different species, and there is a certain degree of difference in water microorganisms between the two sides.



**Figure 8.** The variance analysis of microbial community (genera level)

Table 4 is the Comparison of main dominant categories of microorganisms in Case2 waters. The first dominant bacteria in red tide water and the second dominant bacteria in nearby waters are Proteobacteria. The second dominant bacteria in red tide water and the third dominant bacteria in nearby waters are Bacteroides. However, the proportion of each dominant bacteria is quite different between the two sides. For example, the first dominant bacteria in the red tide area were Proteobacteria (46.1%), accounting for 30.6% in the nearby sea area, while cyanobacteria (42.0%) were the first dominant bacteria in the nearby sea area, accounting for 17.7% in the red tide area.

Huang Bei and other scholars used culturable technology to isolate and purify bacteria from Prorocentrum bloom in the East China Sea and the control waters in Taizhou sea area, and identified the strains based on biochemical reaction <sup>[13]</sup>. The results showed that the dominant bacteria in red tide water were Vibrio and Pseudomonas, all belonging to the Proteobacteria, which was consistent with the survey results. However, the main dominant bacteria in Zhujiajian sea area without red tide are Flavobacterium and Aeromonas, the results of this investigation are cyanobacteria, which are quite different. This is due to the

**Table 4.** Dominant species of marine microbes (phylum level)

	First dominant bacteria	Second dominant bacteria	Third dominant bacteria	Fourth dominant bacteria
HAB01	Proteobacteria, 46.1%	Bacteroidetes, 27.2%	Cyanobacteria, 17.7%	Verrucomicrobia, 1.0%
ZJ0205	Cyanobacteria, 42.0%	Proteobacteria, 30.6%	Bacteroidetes, 21.4%	Actinobacteria, 0.4%.

different technical means used in the second survey. The high-throughput sequencing method used in this survey is quite different from the traditional biochemical identification of bacteria. In addition, the sampling sea area of the two methods is also different, so the results are quite different. According to the 16S rDNA sequence of cultivable bacteria in different periods of red tide, Wang Jian and other scholars carried out molecular classification and identification of bacteria, and found that most of the bacteria are bacterial groups of the Proteobacteria and Bacteroides [14].

Chang Hong and other scholars used molecular biology methods such as terminal restriction fragment length polymorphism (T-RFLP) analysis, through principal component analysis and cloning library construction, to study the bacterial community structure of S. conidus during the red tide in the Shenzhen Dapeng Bay. It was found that the types of bacteria mainly belong to the Proteobacteria, Bacteroides and Firmicutes [15]. Hye Eun Kang and other scholars carried out molecular biology research on the microbial community during the occurrence of Heterosigmaak ashiwo red tide in Juji Island, South Korea. The 16S rDNA sequencing and species identification results showed that Proteobacteria and Bacteroides are the two most important bacterial groups in red tide waters, followed by Firmicutes and Actinomycetes [16]. It can be seen that using molecular biology techniques to study water microbial communities when red tides occur, although the causes of red tides and the studied sea areas are different. the structure of the water microbial community is relatively similar at the phylum level. Proteobacteria, Bacteroides, Actinobacteria and Firmicutes are the main bacterial groups. The results of this study also confirmed this conclusion.

# 3.4 Correlation Analysis of Water Quality and Phytoplankton

In order to directly reflect the correlation between phytoplankton and environmental factors, the Past software and CCA analysis method were used for sequencing. Through the analysis of the correlation between phytoplankton species number, cell abundance, chlorophyll, Shannon index and environmental factors, it was found that the first axis and the second axis explained 93.2% and 5.4% of the total variation respectively in CCA ordination chart (Figure 9), which indicated that the environmental factors in this study explained the variation of phytoplankton community to a great extent. The dots in the figure represent the number of phytoplankton species, cell abundance, chlorophyll, Shannon index, and the rays represent environmental factors.

The dots in the figure represent the number of phytoplankton species, cell abundance, chlorophyll, and Shannon index, and the rays represent environmental factors. The longer the radiation of environmental factors, the greater the impact of the factor on the research object; and the length of the vertical distance from the microorganism to the environmental factors determines the correlation between them, the shorter the distance, the greater the correlation, and the longer the distance, the smaller the correlation. It can be seen from Figure 9 that, in general, the environmental factors in this survey have little effect on the phytoplankton community. For example, each factor has little effect on cell abundance. Relatively speaking, the number of plant species, chlorophyll and Shannon index were significantly affected by active phosphate and

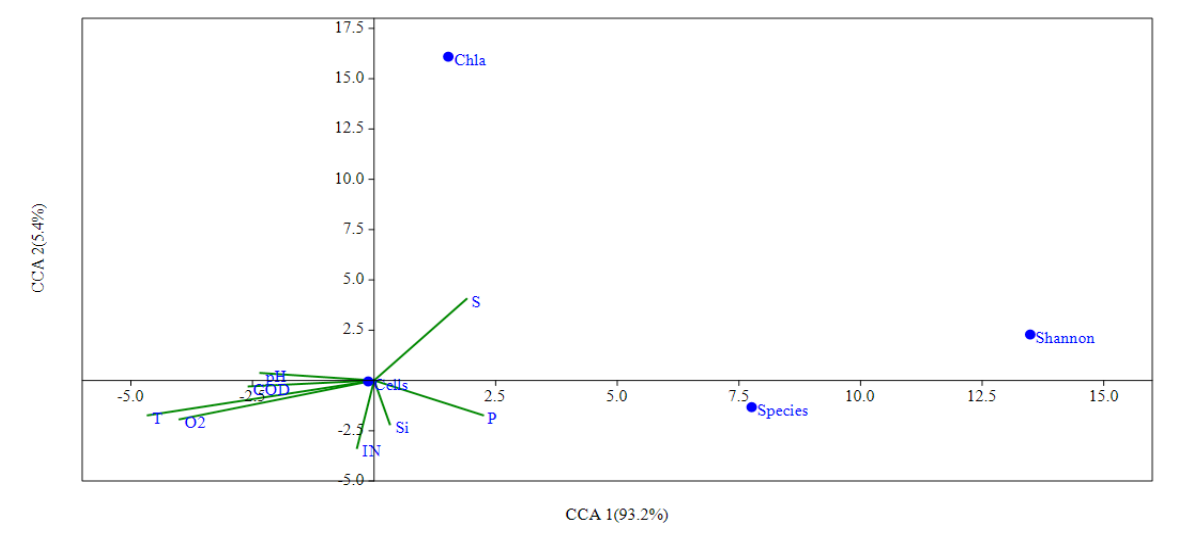


Figure 9. CCA ordination of phytoplankton and environmental factors

salinity in seawater.

Salinity is a key factor in the growth of marine phytoplankton. Dr. Zhang and other scholars studied the phytoplankton and its water quality physical and chemical parameters in Hangzhou Bay in the summer from 2004 to 2010. The survey results showed that salinity was the main variable related to phytoplankton community [17]. In addition, Dr. Jiang and other scholars studied the biomass and physical and chemical indicators of phytoplankton in Xiangshan Bay, Zhejiang Province, and found that phytoplankton also showed spatial heterogeneity along the salinity gradient, which was driven by marine environmental factors [18]. Phosphorus is one of the essential nutrients for the growth of microalgae, and most of the metabolic structure and functions require phosphorus [19,20]. Many scholars have studied the estuarine areas of the East China Sea and the South China Sea, and found that the high nitrogen concentration in the coastal areas of China leads to serious phosphorus limitation [21,22]. The results of this survey are consistent with the above-mentioned research results. In this survey, the concentration of inorganic nitrogen in seawater is generally high, and the CCA ranking shows that active phosphate has a relatively large influence on the number of plant species, chlorophyll, and Shannon index.

### 4. Conclusion

- (1) In June 2018, a patrol survey of the marine ecological environment was carried out in the sea areas with high incidence of red tides along the coast of Zhejiang, China. It was found that the nitrogen and phosphorus nutrient contents in the surveyed seas were generally high, and the inorganic nitrogen of most samples exceeded the first-class sea water quality standards. There are significant differences in dissolved oxygen, pH, COD, chlorophyll and phytoplankton abundance in the water body when red tide occurs. The active phosphate and salinity in seawater have a greater impact on the number of plant species, chlorophyll and Shannon index.
- (2) During the investigation, a red tide was found in the sea area near Yushan Islands. The chlorophyll a content was  $42.12 \text{ mg/m}^3$  and the cell abundance of phytoplankton is  $8.16 \times 10^8 / \text{L}$ , of which the abundance of Prorocentrum donghaiensis accounts for 98.5%. It can be considered that this is a Prorocentrum donghaiense event.
- (3) The Illumina MiSeq sequencing platform was used to perform 16s high-throughput sequencing on the red tide occurrence area and nearby sea waters, and a total of 16 phyla, 82 families and 126 genera of bacteria were identified. At the phylum level, the Proteobacteria is the first dominant phyla, with 38.4% of the total sequence number;

followed by the cyanobacteria and Bacteroides.

(4) Comparing the microbial species composition of the red tide occurrence point and the nearby sea area, there is a certain degree of difference between the two water bodies. The proportion of dominant bacteria between the two groups was quite different. The most dominant bacteria in the red tide area was Proteobacteria, accounting for 46.1%; Cyanobacteria was the first dominant bacteria in the nearby sea area, accounting for 42.0%.

### References

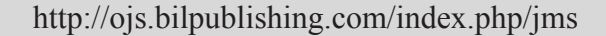
- [1] Mingjiang Zhou, Mingyuan Zhu, Jing Zhang. The trend and research progress of red tides in China[J]. Life Science, 2001(02): 54-59+53. (in Chinese)
- [2] Xiurong Han, Xiulin Wang, Xia Sun, et al. A preliminary study on the distribution characteristics of nutrients in the coastal waters of the East China Sea and their relationship with red tides[J]. The Journal of Applied Ecology, 2003(07): 1097-1101. (in Chinese)
- [3] Jinhui Wang. Red tide organisms in the waters adjacent to the Yangtze River Estuary[J]. Marine Environmental Science, 2002(02): 37-41.
- [4] Ping Xia, Douding Lu, Wei Du, et al. The trend and characteristics of red tide occurrence in Zhejiang coastal waters[J]. Journal of Oceanography, 2007(02): 47-56. (in Chinese)
- [5] Mingjiang Zhou, Mingyuan Zhu. Study on the ecology and oceanography mechanism of harmful red tides in the coastal waters of China and their prediction and prevention[J]. Journal of Applied Ecology, 2003(07): 1029. (in Chinese)
- [6] Doucette G J, Trick C G. Characterization of bacteria associated with different isolates of *Alexandrium tamarense*[A]. Lassus P, Arzul G, Erard E, et al. Harmful Marine Algal Blooms[C]. Paris: Lavoisier Science Publ, 1995. 33-38.
- [7] Sawayama S, Sako Y. Bacterial inhibitions for the mating reaction of Alexandium catenella (Dinophyceae)[A]. Smayda T L, Shimizu Y. Toxic Phytoplankton blooms in the Sea[C]. BV, Amsterdam: Elsevier Sci Publ, 1993. 177-181.
- [8] Arakaki A, Shibusa M, Hosokawa M, et al. Preparation of genomic DNA from a single species of uncultured magnetotactic bacterium by multiple-displacement amplification[J]. Applied and Environmental Microbiology, 2010, 76(5): 1480-1485.
- [9] Gans J, Wolinsky M, Dunbar J. 2005. Computational improvements reveal great bacterial diversity and high metal toxicity in soil. Science, 309(5739):1378-1390.
- [10] Venter J C, Remington K, Heidelberg J F et al. 2004.

- Environmental genome shotgun sequencing of the Sargasso sea[J]. Science, 304(5667): 66-74.
- [11] Bei Huang, Junbo Shao, Bin Zhou, et al. The microbial community in the sediments of Jiaojiang Estuary and its response to environmental factors[J]. China Environmental Monitoring, 2017, 33(06): 87-94. (in Chinese)
- [12] National Environmental Protection Agency. GB3097-1997 Sea Water Quality Standard[S]. Beijing: National Environmental Protection Agency, 1997. (in Chinese)
- [13] Bei Huang, Junbo Shao, Jieyu Wang, et al. Bacteriological study on the occurrence of red tides in the East China Sea[J]. Journal of Water Ecology, 2013, 34(06): 47-51. (in Chinese)
- [14] Jian Wang, Zhaohui Wang, Yijun Xiong. Study on the cultivable inter-algal bacteria of G. striata in different periods[J]. China Environmental Science, 2014, 34(06): 1540-1547. (in Chinese)
- [15] Hong Chang, Bo Wang, Mimi Yao. Study on the changes of bacterial community structure during the red tide of S. conifer in Shenzhen Dapeng Bay[J]. Progress in Modern Biomedicine, 2014, 14(10): 1801-1807. (in Chinese)
- [16] Hye-Eun Kang, Tae-Ho Yoon, Sunyoung Yoon, et al. Genomic analysis of red-tide water bloomed with *Heterosigma akashiwo* in Geoje[J]. PeerJ.4854,2018, DOI 10.7717/peerj.4854 2/25.

- [17] Yuexia Zhang, Jun Yu, Zhibing Jiang, et al. Variations of summer phytoplankton community related to environmental factors in a macro-tidal estuarine embayment, Hangzhou Bay, China[J]. Journal of Ocean University of China, 2015 14 (6): 1025-1033.
- [18] Zhibing Jiang, Xuyu Zhu, Yu Gao, et al. Spatio-temporal distribution of net-collected phytoplankton community and its response to marine exploitation in Xiangshan Bay[J]. Chinese Journal of Oceanology&Limnology, 2013.
- [19] Karl, D.M.. Microbially mediated transformations of phosphorus in the sea: new views of an old cycle. Ann. Rev. Mar. Sci., 2014, 6: 279-337.
- [20] Lin, S., Litaker, R.W., Sunda, W.G. Phosphorus physiological ecology and molecular mechanisms in marine phytoplankton. J. Phycol., 2016, 52(1), 10-36.
- [21] Glibert, P.M., Al-Azri, A., Icarus Allen, J., Bouwman, A.F., Beusen, A.H.W., Burford, M.A., Harrison, P.J., Zhou, M.. Key Questions and Recent Research Advances on Harmful Algal Blooms in Relation to Nutrients and Eutrophication. Global Ecology and Oceanography of Harmful Algal Blooms, 2018: 229-259.
- [22] Yin, K., Harrison, P.J. Nitrogen over enrichment in subtropical Pearl River estuarine coastal waters: possible causes and consequences. Cont. Shelf Res., 2008, 28(12): 1435-1442.



### **Journal of Marine Science**





### ARTICLE

# Mass Spectrometry-based Sequencing of Venom Peptides (Conotoxins) from Vermivorous Cone Snail, Conus Loroisii: Toxicity of its Natural Venom

### Humaira Saleh Syed<sup>2</sup> Rishimol R<sup>2</sup> Arun Kumar J<sup>2</sup> M Masilamani Selvam<sup>3</sup> Rajesh R P<sup>1\*</sup>

- 1.Molecular and nanomedicine Research Unit, Centre for nanoscience and nanotechnology, Sathyabama Institute of Science and Technology, Chennai, 600119, Tamil Nadu, India
- 2.Department of biotechnology, Dr. M.G.R. Educational and research institute, Maduravoyal, Chennai, 600095, Tamil Nadu, India
- 3. Department of Biotechnology, Sathyabama Institute of Science and Technology, Chennai, 600119, Tamil Nadu, India

#### ARTICLE INFO

Article history

Received: 23 September 2020 Accepted: 5 November 2020 Published Online: 31 January 2021

Keywords: Conus loroisii Conotoxins Toxicity

Mass spectrometry

#### ABSTRACT

Conus loroisii is a marine vermivorous snail found profusely in the southern seas of India. They harbor several toxic peptide components commonly called as 'conotoxins'. In this study, we have identified and sequenced five conotoxins using proteome based tandem mass spectrometry analysis through Data analysis 4.1 software. Among them, we found Lo959 as contryphan which is previously described. All other conotoxins Lo1702, Lo1410, Lo1385 and Lo1686 belong to M-Superfamily conotoxins and novel to C. loroisii. Lo1410 is completely novel to conotoxin research with 3 disulfides and the amino acid sequence is derived as CCSTNCAVCIPCCP. All the identified M-Superfamily conotoxins are sub categorised to mini M2 superfamily conotoxins. Lo1702 and Lo1686 possess C- terminal amidation which is the key feature in conotoxins. Moreover, we have screened the natural venom for the occurrence of toxicity in the zebrafish model and brine shrimp.

### 1. Introduction

Cone snails form the largest single genera of living marine invertebrates and include various carnivorous predators. Conidae, commonly known as 'cone snails', is a taxonomic family of predatory sea snails and marine gastropod molluscs belonging to the genus Conus established as a family by John Flemming in 1822. The Conidae along

with the Turridae and Terebridae form the Superfamily Conidia [1]. These marine gastropod genus Conus (cone snails) found mainly in shallow waters around the world. The genus Conus is rich in diversity found in almost all parts of tropical seas which makes this as important in marine diversity and also play a major role in economy for its beautiful shells. As cone snails possess venom cocktail which majorly act in the prey's neuronal system,

Rajesh R P,

Molecular and nanomedicine Research Unit, Centre for nanoscience and nanotechnology, Sathyabama Institute of Science and Technology, Chennai, 600119, Tamil Nadu, India;

E-mail: jeshran@gmail.com.

<sup>\*</sup>Corresponding Author:

which primarily serves to capture prey is now a days developed as neurological drugs and tools. A venom peptide from Conus magus Ziconotide is the first approved drug from a marine gastropod which is used in chronic pail alleviation [2]. From that point several other library of conotoxins is continuously studied for their medicinal properties isolated from several conotoxins worldwide [3]. The venom of all classes of conotoxins from various cone snails are highly unique in their structure and function [4]. Despite cone snails are widely used through exploitation for their commercial, medical and scientific value, very less research has been focused towards the conservation of the genus Conus. Based on feeding habits conus is classified in to piscivorous which hunt fish, molluscivorous which feeds mollusk and vermivorous which hunts on worms. Among them piscivorous which hynt fishes is the remarkable group as these venom has potential to target vertebrate system and it normally used to rapidly immobilize fish [5].

Few conotoxins have reached human clinical trials; many are at preclinical stages of development for diverse potential therapeutic applications.

Only very few percentage of the whole conotoxins identified have been studied and developed for medical applications <sup>[6]</sup>. Cone snails which harbor cocktail of potential conotoxins, serve as a big reservoir for development of several marine drugs. Most of these toxins have been found to exhibit potential bioactivity in a diverse range of mammalian ion channels and receptors associated with pain-signaling pathways.

Typically the conotoxins are of small size, with well-defined stable structure, highly specific towards the target receptors make them attractive and potential pharmacologic agents.

Many conotoxins have shown promise and potential in preclinical models of pain, convulsive disorders, stroke, neuromuscular block, and cardioprotection.

Most conopeptides families studied to date target receptors and ion channels associated with muscle tissue and nervous system.

Some conotoxins which have specific function of alleviation of pain are developed as pain killers [7]. In this study, we have characterized few of the venom peptides using mass spectrometry based studies and biological characterization of the venom using the zebrafish model.

### 2. Materials and Methods

### 2.1 Collection and Identification of Cone Snail

Conus loroisii samples were collected from Kasimedu fishing harbor (13.1251° N, 80.2955° E), (Figure 1a),

Tamil Nadu, India. A total of 22 alive C. loroisi samples were collected from the trawling fish waste littered in the boat jetty of Kasimedu fishing harbor in the month of January, 2019. The collected cone snail was identified following standard keys<sup>[8]</sup>. We selected C. loroisii for this study as is not enlisted under endangered or protected species.



**Figure 1a.** Map showing sampling location of conus loroisii at Kasimedu fishing harbor



Figure 1b. Shell and venom duct of conus loroisii

### 2.2 Extraction of Natural Peptides

The venom ducts of C. loroisii specimens were dissected and stored in 50: 50 % HPLC grade acetonitrile: water at the collection site. The samples were transported to the laboratory and the crude natural extract was filtered through Whatman No.1 filter paper and the clean filtrate was concentrated using a rotary vacuum evaporator. The crude extract was then stored at -20 °C till further use <sup>[9]</sup>.

### 2.3 LC-MS-MS of the Natural Extract

The crude extract of C. loroisii was filtered through a  $0.2\mu M$  filter and diluted and subsequently, used for mass spectrometric analysis. The mass spectrometric data was acquired in LC-MS-MS (Bruker Daltonics, Bremen, Ger-

many) to identify the number of peptide components in the crude mixture [9].

# **2.4** Global Reduction and Alkylation of Natural Venom and Analysis by LC-MS-MS

An aliquot of crude venom extract was treated with reducing agent TCEP (tris (2-carboxyethyl) phosphine) at a final concentration of 20mM and incubated at 37 °C for 1.5 h. After incubation double the concentration (40mM) of alkylating agent NEM (N-Ethyl maleimide) was added and incubated at room temperature for 45min. The reaction mixture was analyzed in LC-MS-MS to identify the number of disulfide-rich conopeptide <sup>[9]</sup>. Auto MS (n) experiments (CID fragmentation) was performed for the reduced and alkylated peptides. All the above experiments are carried after the peptide components were chromatographically separated based on their polarity using a reverse phase C18 column <sup>[9]</sup>.

### 2.5 Sequencing of Venom Peptides

Manual de novo sequencing strategy was followed to sequence the conotoxins from the raw data obtained from LC-MS-MS using Data analysis 4.1 software (Bruker Daltonics, Bremen, Germany).

### 2.6 Toxicity Testing of Conotoxin on Zebrafish Embryos

Adult and healthy zebrafish were obtained and maintained in a standalone system (Aquaneering, USA) 25-28°C, under 14–10 h light/dark cycle photoperiod in 50 L housing tank. 6 hpf (hours post fertilization) healthy embryos were screened without any visible physical defects and developmental deformities. The zebrafish embryos were exposed to the Conotoxins (100, 200, 400, 600, 800,  $1000\mu g/mL$ ) for 6-72 hpf and then assessed for toxicity. The embryos were kept in sterile 24-well plates with 10 embryos per well-containing 1mL of the solution. The mortality and developmental deformities of the zebrafish larvae were recorded at 72 hpf (hour post-fertilization) [10, 11, 12].

### 2.7 Toxicity Assay of Crude Venom on Brine Shrimp

Artemia salina (brine shrimp) eggs were purchased from Ocean Star International O.S.I, USA. Dried cysts were placed in a separating funnel containing natural seawater. After 24-28 hours of incubation and strong aeration at room temperature (30-35° C) under continuous light supply, the nauplii (larvae) were hatched. The larvae were separated using a coffee filter and rinsed well in sterile seawater. The nauplii were then suspended in sterile seawater.

The evaluation of cytotoxicity on the brine shrimp embryo was performed by adding 10 larvae in each well containing 100 µl of sterile seawater. The test was performed in triplicates. The larvae were exposed to different concentration of drug (5, 10, 20, 40, 80, 160, 320µg/mL). After 24 hours of incubation at room temperature, the number of nauplii surviving was checked under a stereo microscope. The control well consisted of only nauplii and sterile seawater. The percentage of deaths was calculated by comparing the test and control wells. The percentage of lethality was calculated by means of Abbott's formula: % Lethality= ((Test-Control)/ Control) \* 100 [13].

### 2.8 Acetylcholinesterase Quantification

The acetylcholinesterase quantification assay was performed in 96-well plate to which different concentrations of conotoxin was added and made up to  $250\mu l$  with PB buffer (pH 7) for 10 mins at room temperature. After incubation, the reaction was stopped by addition of Tris HCl (pH 8). Then  $10~\mu l$  of 5, 5'-dithiobis (2-nitrobenzoic acid) (DTNB) was added to each well and absorbance was taken at 412 nm.  $2~\mu l$  of acetyl thiocholine iodide was added to each well to measure the hydrolysis of ATCI by formation of yellow reaction of DTNP with thiocholine and the reaction was measured by 412 nm in multi-mode plate reader (PerkinElmer)  $^{[10,11,12]}$ .

#### 3. Results

### 3.1 Identification, Dissection and Isolation of Crude Venom from Conus Loroisii

The cone snail was identified following standard keys as Conus loroisii (Figure 1). The venom duct was dissected from the live specimen (Figure 1). Venom is extracted from the venom duct by following the protocol as given in materials and methods and stored in the deep freezer (-20°C) for preservation until further use. The presence of protein in the crude venom extract was confirmed using NanoDrop (Thermo Scientific<sup>TM</sup> NanoDrop 2000 and 2000c) and its concentration was 3 mg/ml.

#### 3.2 Sequencing of Venom Peptides

The total ion chromatogram of C. loroisii venom yielded a spectrum showing various peptide components. Among them, we identified and sequenced five peptides Lo959, Lo1702, Lo1686, Lo1410 and Lo1385 respectively. The fragmented spectrum of Lo959, Lo1702, Lo1686, Lo1410, and Lo1385 with daughter ions which are exclusively used for deriving the peptide sequences are shown in figure 2-6 respectively. The individual masses

of both the 'b' and 'y' series where determined manually by de-novo sequencing and are presented in the tables (2-6). Complete analysis of the daughter ions yielded the sequences Lo959- GCPWDPWC-NH2, Lo1702-CCSQD-CRVCIOCCPY-NH2, Lo1686- CCSQDCRVCIPC-CPY-NH2, Lo1410- CCSTNCAVCIPCCP, and Lo1385-CCKVLCESCTPCC. ExceptLo959 all other peptide toxins are novel to be reported from C. loroisii. Peptide

Lo959 belongs to the contryphan family. The other four sequences Lo1702, Lo1686, Lo1410 and Lo1385 belong to the M superfamily of conotoxins. The MALDI-TOF spectrum of two conotoxins Lo1686 and Lo1702, after alkylation, was determined and it indicates the post translational modification that takes place between Lo1686 and Lo1702. A difference of 16 Dalton between both the peptides is noted.

Table 1. Conopeptides of conus loroisii

Sl. No.	Gene Superfamily	Name	Sequence	Mass	Notes
1	Contryphan	Lo959	GCPWDPWC-NH2	959	This Work and Gowd,K.H. et al. (2005) Sabareesh,V. et al. (2006) Sonti,R. et al. (2013)
2	M-superfamily	Lo1702	CCSQDCRVCIOCCPY-NH2	1701	This Work and Rajesh 2014
3	M-superfamily	Lo1410	CCSTNCAVCIPCCP	1409	Novel to conotoxins history
4	M-superfamily	Lo1385	CCKVLCESCTPCC	1384	Peng C et al., 2016
5	M-superfamily	Lo1686	CCSQDCRVCIPCCPY-NH2	1685	Conticello et al 2001 and Rajesh 2014

Table 2. Determined m/z values of b and y ions for the sequence Lo959

b ions	Theoretical Mass	Founded Mass	y ions	Theoretical Mass	Founded Mass
b1	59		yl	246	
b2	287		y2	432	
b3	384		у3	529.35	529.35
b4	570	570	y4	644.3	644.3
b5	685	685	у5	830	
b6	781		у6	927.47	927.47
b7	967.47	967.47	у7	1155	

**Table 3.** Determined m/z values of b and y ions for the sequence Lo1702

b ions	Theoretical Mass	Founded Mass	y ions	Theoretical Mass	Founded Mass
b1	229		y1	182	
b2	457.3	457.3	y2	279	
b3	544.1		y3	507.2	507.2
b4	672.2		y4	735.1	735.1
b5	787.4	787.4	y5	848.3	848.3
b6	1015.3	1015.3	y6	961.4	961.4
b7	1171.3		у7	1189.5	1189.5
b8	1270.5	1270.5	y8	1104	1104
b9	1498.5	1498.5	у9	1445.4	1445.4
b10	1611.6		y10	1672.7	1672.7
b11	1724.9	1724.9	y11	1787.6	
b12	1952.6	1952.6	y12	1915.7	
b13	2180.7	2180.7	y13	2002.5	2002.5
b14	2277.6		y14	2230.5	

Table 4. Determined m/z values of b and y ions for the sequence Lo1410

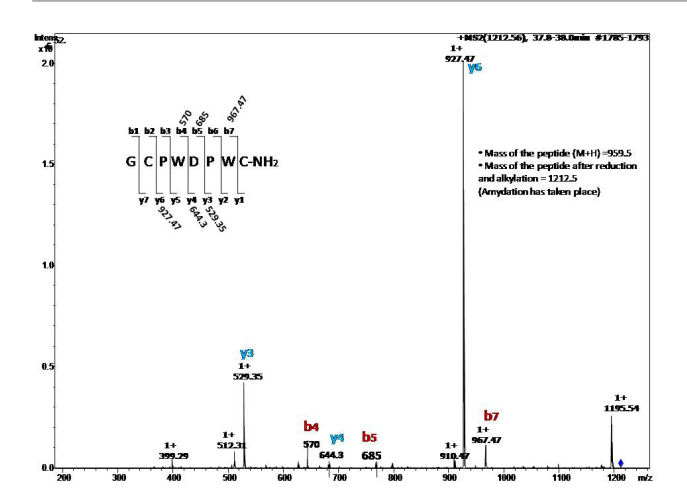
b ions	Theoretical Mass	Founded Mass	y ions	Theoretical Mass	Founded Mass
b1	229		y1	116	
b2	457	457	y2	344	344
b3	544	544	y3	572	572
b4	645	645	y4	669	669
b5	759.4	759.4	у5	782	782
b6	987.3	987.3	y6	1010	1010
b7	1058.4	1058.4	у7	1109	1109
b8	1157.4	1157.4	y8	1180	1180
b9	1385.5	1385.5	у9	1408	1408
b10	1498	1498	y10	1522	1522
b11	1595.6	1595.6	y11	1623	
b12	1823.7	1823.7	y12	1710	
b13	2051.7		y13	1938	

Table 5. Determined m/z values of b and y ions for the sequence Lo1384

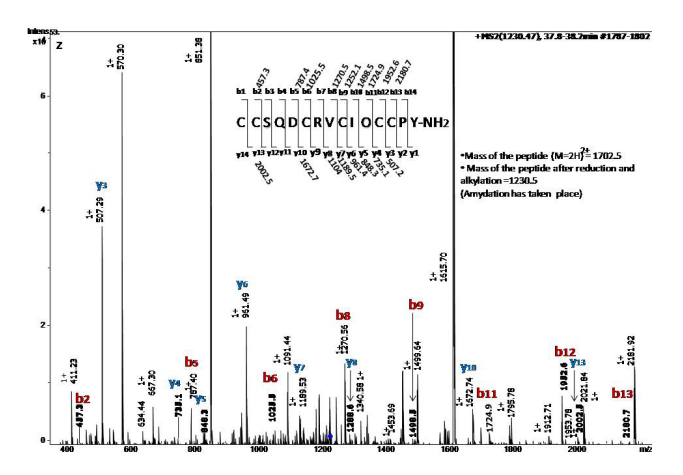
b ions	Theoretical Mass	Founded Mass	y ions	Theoretical Mass	Founded Mass
b1	229		y1	475.2	475.2
b2	457	457	y2	572.3	572.3
b3	585	585	y3	673.3	673.3
b4	684.3	684.3	y4	901	901
b5	797.5	797.5	у5	988.4	988.4
b6	1025.5	1025.5	y6	1117	
b7	1154	1154	у7	1345.5	1345.5
b8	1241.6	1241.6	y8	1458	1458
b9	1469.6	1469.6	у9	1557	
b10	1570.7	1570.7	y10	1656	
b11	1667.7	1667.7	y11	1784	
b12	1895.7	1895.7	y12	2012	

Table 6. Determined m/z values of b and y ions for the sequence Lo1686

b ions	Theoretical Mass	Founded Mass	y ions	Theoretical Mass	Founded Mass
b1	229		y1	182	
b2	457	457	y2	279	
b3	544		у3	507	507
b4	672	672	y4	735	
b5	787	787	у5	832	832
b6	1015		у6	945	945
b7	1171	1171	у7	1173	1173
b8	1270	1270	у8	1272	1272
b9	1498	1498	у9	1428	1428
b10	1611	1611	y10	1656	1656
b11	1708	1708	y11	1771	1771
b12	1936	1936	y12	1899	
b13	2164	2164	y13	1986	
b14	2067		y14	2214	



**Figure 2.** Spectrum showing sequence of Lo959 obtained from de novo tandem Mass Spectrometry



**Figure 3.** Spectrum showing sequence of Lo 1702 obtained from de novo tandem Mass Spectrometry (O= 4-trans-hydroxyproline: Hyp)

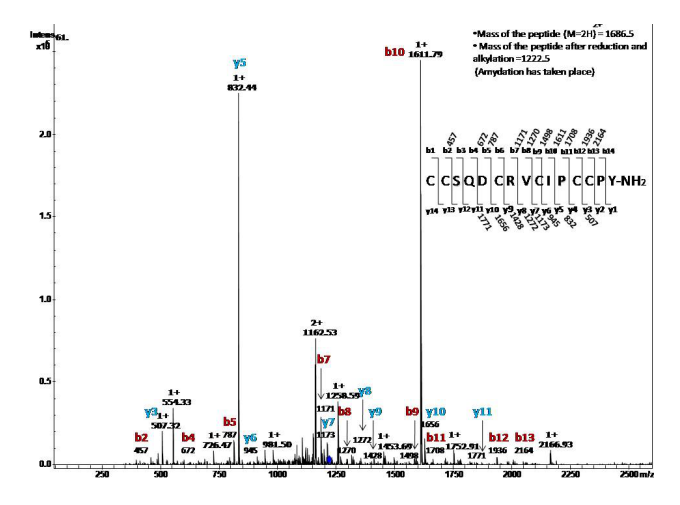


**Figure 4.** Spectrum showing sequence of Lo 1686 obtained from de novo tandem Mass Spectrometry

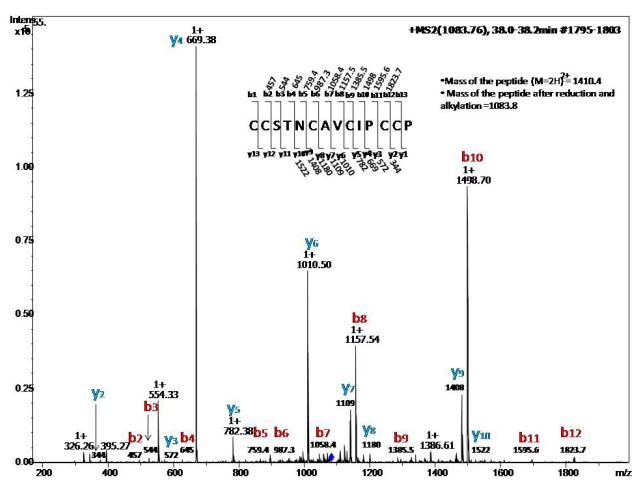


**Figure 5.** Spectrum showing sequence of Lo 1410 obtained from de novo tandem Mass Spectrometry

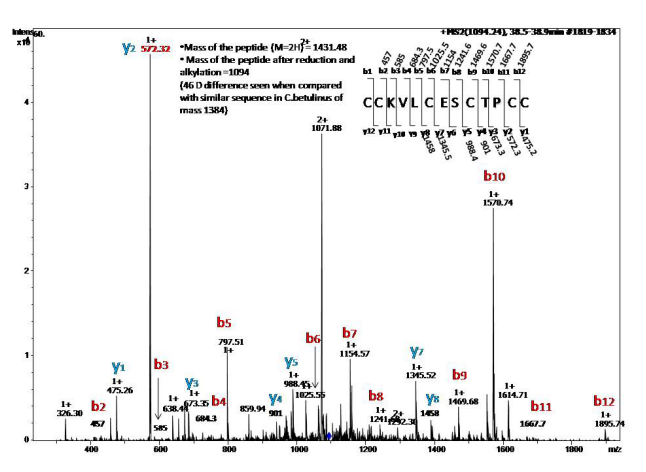


**Figure 6.** Spectrum showing sequence of Lo 1385 obtained from de novo tandem Mass Spectrometry

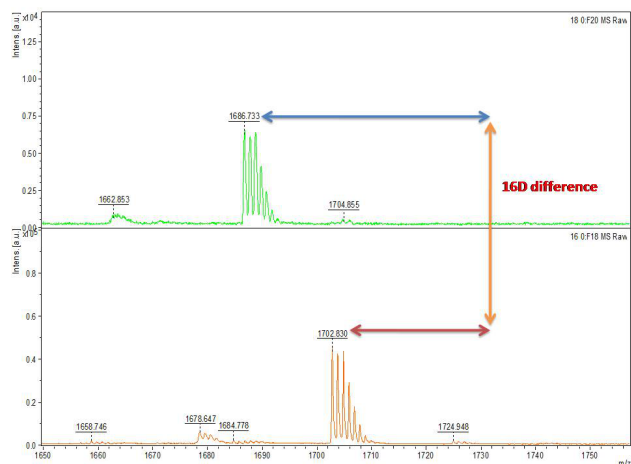


**Figure 7.** Spectrum showing sequence of Lo 1686 and Lo1702 with 16D more indicating the presence of hydroxyl proline in Lo1702

### 3.3 Estimation of Acetylcholinesterase Activity

The venom sample was tested for the presence of acetylcholinesterase enzyme using the Ellman's assay (as described in detail in materials and methods). We observed that the venom sample of Conus loroisii contains the enzyme acetylcholinesterase as shown in Figure 8.

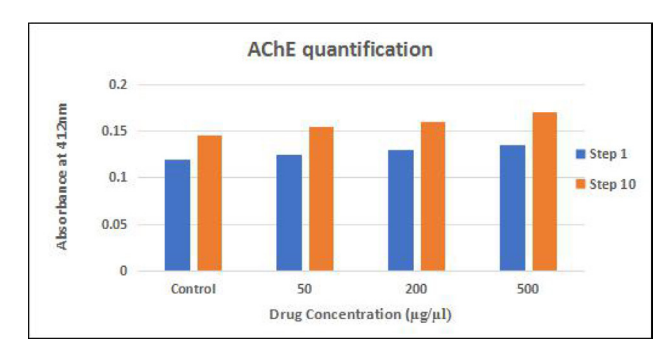


**Figure 8.** Quantification of the enzyme acetylcholinesterase

# 3.4 Toxicity Testing of Conotoxin on Zebrafish Embryos

Zebrafish embryos were subjected to varying concentrations of conotoxins for 72 h.p.f based on OECD guidelines to determine the LC50 value. It was observed that death was initiated at a concentration of 400  $\mu$ g/ $\mu$ l at 24 hrs. Between 50-65 hours after treatment, various deformities were observed in higher concentrations such as pericardial edema, blood clot, yolk sac edema, spinal kyphosis, etc. 100% death was observed in concentration 800  $\mu$ g and above (Figure 9&10). The LC50 was determined to be 700  $\mu$ g/ $\mu$ l with 50% death.

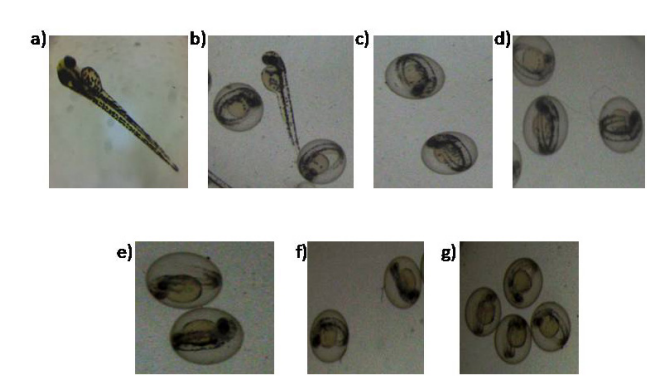


**Figure 9.** Toxicity assessment of zebrafish embryo at 24 hours post treatment (hpt) a) Control; b) 100μg; c) 200μg; d) 400μg; e) 600μg; f) 800μg; g) 1000μg









**Figure 10.** Different deformities observed in the zebrafish larvae during toxicity assessment vs control. a)Control b) Pericardial edema; c) Hemorrhage; d) Spinal kyphosis (Deformities seen at 48 & 72 hrs.)

### 3.5 Toxicity Assay of Crude Venom on Brine Shrimp

Brine shrimp toxicity was performed on 24hrs nauplii at varying concentrations of conotoxins for 24 h.p.f as mentioned in materials and methods. It was observed that death was initiated at a concentration of  $80 \mu g/\mu l$ . The LC50 value was found to be  $320\mu g/\mu l$  at 24 hours.

### 4. Discussion

Conus loroisii is abundantly distributed along the coast of the Southeastern state of Tamil Nadu in India. Despite its abundance, the venom components of this species have not been studied extensively. The de-novo sequencing done with the help of mass spectrometry has led to yield five peptide sequences. Among these peptides, one was found to be a contryphan and the other four belong to the M-superfamily conotoxin. One contryphan (Lo959) and two peptides from the M-superfamily Lo1385 [13] and Lo1686 [9] identified in this study have been identified earlier in other cone snails (Conus betulinus and Conus figulinus). Two peptides from the M-superfamily (Lo1702 and Lo1410) are novel toxins to the conopeptide library. Several conotoxins with from Conus amadis displayed almost similar sequence similarity with the peptide sequence of the present study (Vijayasarathy et al., 2019). Among the 5 conotoxins identified 3 peptides possess C terminal amidation which is the major hallmark of conotoxins. Lo1702 possess the hydroxylation of proline which is another major post-translational modification which also found in Conus figulinus as reported earlier [9]. The LC50 value was determined to be 700 µg/µl by zebrafish embryo toxicity and 320 µg/µl by brine shrimp toxicity. The conotoxin lacked acetylcholinesterase inhibitory activity but helps in increasing the activity of acetylcholinesterase. Based on the preliminary evidence for the occurrence of novel conotoxins and the toxicity studies, if this study is extended further and trace out and separate the toxigenic molecules, which would provide a lead for discovering biologically active molecules.

### 5. Conclusion

In this study the vermivorous cone snail Conus loroisi which is less explored for its venom based peptidomic research is analysed using mass spectrometry based de-novo sequencing and tested for its toxicity in zebrafish model and brine shrimp. We found 5 peptides and derived their aminoacid sequences, which belong to single disulfide contryphan group and 3 disulfide bonded M-superfamily conotoxins. Among them Lo1410 is completely novel to conotoxin research. This preliminary research paved the way to continue research in biological and structural characterisation of individual peptide molecules which would possibly yield us with drug leads against various human ailments in near future.

Funding: In house funding

Conflict of Interest: The authors declare no conflict of

interest.

### Acknowledgments

All authors thank Sathyabama Institute of Science and Technology for laboratory support to carry out experiments.

#### **Abbreviations**

LC-MS-MS, Liquid Chromatography-Mass Spectrometry- Mass Spectrometry;

TCEP, tris (2-carboxyethyl) phosphine [Pierce Scientific, United States];

NEM, N-Ethylmaleimide [Sigma-Aldrich, United States];

CID, Collision-induced dissociation;

MS, Mass Spectrometry;

hpf, Hours post fertilization;

AChE, Acetylcholinesterase;

dpf, days post fertilization;

E3, Embryo medium;

DMSO, Dimethyl sulfoxide;

TIC, Total Ion Chromatogram;

Da, Dalton

### References

- [1] Röckel, D., Korn W, Kohn, A.J. Manual of the Living Conidae. Wiesbaden, Hemmen. 1995.
- [2] Staats, Peter S., Thomas Yearwood, Steven G. Charapata, Robert W. Presley, Mark S. Wallace, Michael Byas Smith, Robert Fisher. Intrathecal ziconotide in the treatment of refractory pain in patients with can-

- cer or AIDS: a randomized controlled trial. JAMA, 2004. 1: 63-70.
- [3] Bruce, G., Livett David, W., Sandall, David Keays, John Down, Ken R. Gayler, Narmatha Satkunanathan, Zeinab Khalil. Therapeutic applications of conotoxins that target the neuronal nicotinic acetylcholine receptor, Toxicon, 2006, 48(7): 810-829. https://doi.org/10.1016/j.toxicon.2006.07.023Get rights and content
- [4] Olivera, B.M., Walker, C., Cartier, G.E., Hooper, D., Santos, A.D., Schoenfeld, R., Shetty, R., Watkins, M., Bandyopadhyay, P., Hillyard, D.R. Specification of cone snails and interspecific hyperdivergence of their venom peptides. Potential evolutionary significance of introns, Ann. N.Y. Acad. Sci., 1999, 870: 223.
- [5] Kaas, Quentin. Conopeptide Characterization and Classifications: An Analysis Using Cono Server. Toxicon, 2010, 55(8): 1491-1509.
- [6] Olivera, B.M., Showers Corneli, P., Watkins, M., Fedosov, A. Biodiversity of Cone Snails and other Venomous Marine Gastropods: Evolutionary Success through Neuropharmacology. Annual Review of Animal Biosciences, 2014, 2: 487-513.
- [7] McIntosh, J.M., Olivera, B.M., Cruz, L.J., Conus peptides are probes for ion channels. Methods in Enzymology, 1999, 294: 605-624. https://doi.org/10.1016/S0076-6879(99)94034-X
- [8] Franklin, J., Benjamin, K.A., Subramanian, S., Antony Fernando, Krishnan, K.S. Diversity and distribution of conidae from the Tamil Nadu coast of India (Mollusca: Caenogastropoda: Conidae). Zootaxa, 2009, 2250: 3-63.
- [9] Rajesh, R. P. Novel M-Superfamily and T-Superfamily conotoxins and contryphans from the vermivorous snail Conus figulinus, Journal of Peptide Science, 2014, 21: 29–39.

https://doi.org/10.1002/psc.2715

- [10] Kumar, A., Bhardwaj, M., Kaur, H. Possible role of neuroprotectants and natural products in epilepsy: Clinical aspects and mode of action, neuroprotective natural products, 2017, 2: 247-277.
- [11] Schmidt, D. Antiepileptic Drugs. Handbook of Experimental Pharmacology. Springer, 1985, 74: 791-829.
- [12] Lamthanh, Hung, Christelle Jegou-Matheron, Denis Servent, André Ménez, Jean-Marc Lancelin. Minimal conformation of the α-conotoxinImI for the α7 neuronal nicotinic acetylcholine receptor recognition: correlated CD, NMR and binding studies. FEBS letter, 1999, 454 (3): 293-298.
- [13] Jackson, Helen, C., Mark, A., Scheideler. Behavioral and anticonvulsant effects of Ca 2+ channel toxins in DBA/2 mice. Psychopharmacology, 1996, 126 (1): 85-90.

### **Author Guidelines**

This document provides some guidelines to authors for submission in order to work towards a seamless submission process. While complete adherence to the following guidelines is not enforced, authors should note that following through with the guidelines will be helpful in expediting the copyediting and proofreading processes, and allow for improved readability during the review process.

### I. Format

Program: Microsoft Word (preferred)

• Font: Times New Roman

• Size: 12

• Style: Normal

Paragraph: Justified

Required Documents

### II. Cover Letter

All articles should include a cover letter as a separate document.

The cover letter should include:

• Names and affiliation of author(s)

The corresponding author should be identified.

Eg. Department, University, Province/City/State, Postal Code, Country

• A brief description of the novelty and importance of the findings detailed in the paper

Declaration

v Conflict of Interest

Examples of conflicts of interest include (but are not limited to):

- Research grants
- Honoria
- Employment or consultation
- Project sponsors
- Author's position on advisory boards or board of directors/management relationships
- Multiple affiliation
- Other financial relationships/support
- Informed Consent

This section confirms that written consent was obtained from all participants prior to the study.

• Ethical Approval

Eg. The paper received the ethical approval of XXX Ethics Committee.

Trial Registration

Eg. Name of Trial Registry: Trial Registration Number

Contributorship

The role(s) that each author undertook should be reflected in this section. This section affirms that each credited author

has had a significant contribution to the article.

1. Main Manuscript

2. Reference List

3. Supplementary Data/Information

Supplementary figures, small tables, text etc.

As supplementary data/information is not copyedited/proofread, kindly ensure that the section is free from errors, and is

presented clearly.

III. Abstract

A general introduction to the research topic of the paper should be provided, along with a brief summary of its main

results and implications. Kindly ensure the abstract is self-contained and remains readable to a wider audience. The

abstract should also be kept to a maximum of 200 words.

Authors should also include 5-8 keywords after the abstract, separated by a semi-colon, avoiding the words already used

in the title of the article.

Abstract and keywords should be reflected as font size 14.

W. Title

The title should not exceed 50 words. Authors are encouraged to keep their titles succinct and relevant.

Titles should be reflected as font size 26, and in bold type.

**IV.** Section Headings

Section headings, sub-headings, and sub-subheadings should be differentiated by font size.

Section Headings: Font size 22, bold type

Sub-Headings: Font size 16, bold type

Sub-Subheadings: Font size 14, bold type

Main Manuscript Outline

V. Introduction

The introduction should highlight the significance of the research conducted, in particular, in relation to current state of

research in the field. A clear research objective should be conveyed within a single sentence.

**VI.** Methodology/Methods

In this section, the methods used to obtain the results in the paper should be clearly elucidated. This allows readers to be

able to replicate the study in the future. Authors should ensure that any references made to other research or experiments

should be clearly cited.

**W**. Results

In this section, the results of experiments conducted should be detailed. The results should not be discussed at length in

this section. Alternatively, Results and Discussion can also be combined to a single section.

### **III.** Discussion

In this section, the results of the experiments conducted can be discussed in detail. Authors should discuss the direct and indirect implications of their findings, and also discuss if the results obtain reflect the current state of research in the field. Applications for the research should be discussed in this section. Suggestions for future research can also be discussed in this section.

### IX. Conclusion

This section offers closure for the paper. An effective conclusion will need to sum up the principal findings of the papers, and its implications for further research.

### X. References

References should be included as a separate page from the main manuscript. For parts of the manuscript that have referenced a particular source, a superscript (ie. [x]) should be included next to the referenced text.

[x] refers to the allocated number of the source under the Reference List (eg. [1], [2], [3])

In the References section, the corresponding source should be referenced as:

[x] Author(s). Article Title [Publication Type]. Journal Name, Vol. No., Issue No.: Page numbers. (DOI number)

### **XI.** Glossary of Publication Type

J = Journal/Magazine

M = Monograph/Book

C = (Article) Collection

D = Dissertation/Thesis

P = Patent

S = Standards

N = Newspapers

R = Reports

Kindly note that the order of appearance of the referenced source should follow its order of appearance in the main manuscript.

Graphs, Figures, Tables, and Equations

Graphs, figures and tables should be labelled closely below it and aligned to the center. Each data presentation type should be labelled as Graph, Figure, or Table, and its sequence should be in running order, separate from each other.

Equations should be aligned to the left, and numbered with in running order with its number in parenthesis (aligned right).

### XII. Others

Conflicts of interest, acknowledgements, and publication ethics should also be declared in the final version of the manuscript. Instructions have been provided as its counterpart under Cover Letter.

### **About the Publisher**

Bilingual Publishing Co. (BPC) is an international publisher of online, open access and scholarly peer-reviewed journals covering a wide range of academic disciplines including science, technology, medicine, engineering, education and social science. Reflecting the latest research from a broad sweep of subjects, our content is accessible world-wide——both in print and online.

BPC aims to provide an analytics as well as platform for information exchange and discussion that help organizations and professionals in advancing society for the betterment of mankind. BPC hopes to be indexed by well-known databases in order to expand its reach to the science community, and eventually grow to be a reputable publisher recognized by scholars and researchers around the world.

BPC adopts the Open Journal Systems, see on ojs.bilpublishing.com

### **Database Inclusion**



Asia & Pacific Science Citation Index



Google Scholar



Creative Commons



Crossref



China National Knowledge Infrastructure



MyScienceWork



Tel:+65 65881289
E-mail:contact@bilpublishing.com
Website:www.bilpublishing.com